

東方電氣評論



2021

35 1 137
1987

东方电气评论



编辑委员会

主任委员：王为民

副主任委员：王政 杨永

委员：马擎天 王晓亮 王 愚 王建录 王拯元

方 宇 邓仲勇 乐劲松 石清华 光海杰

刘世洪 刘泰生 张启 张 杰

杨华 生 建 永 世

建华 杰 洪

光

杨永

主：东方电气
主编：王为民

副主编：王政 杨永

任编辑：王为民

编辑：王为民

编辑：《东方电气》

18

：611731

：028-87898262/63

：028-87898267

：dfdqpl@dongfang.com

地址：成都

邮编：610017

电话：782

简介 (1)

层 (5)

..... (9)

50 MVar (13)

EL-CI (17)

..... (22)

..... (2)

..... (30)

..... (34)

..... (40)

..... (45)

..... (49)

..... (55)

..... 58

T I 1

..... (65)

..... 70

..... 73

..... (77)

..... (85)

..... (21)(33)(44)(0)(88)

[JCN51-1333/TM*1987*q*A4*88*zh*p*¥8.00*750*20*2021-01

CONTENTS



BASIC RESEARCH

- Modal Test and Simulation of Nine-tube Prototype of Liquid Sodium Heat Exchanger *PENG Fan, WANG Liwen, ZHENG Wu, et al*(1)
 Analysis of Soil Remediation Technology *TIAN Jian, WU Jiahua, HU Chunyun, et al*(5)
 Study on the Effect of Cracks in Catalyst Layer on the Durability of PEMFC Membrane Electrode Assembly *XIE Guangyou, ZHU Leifeng, LI Ting*(9)

THERMAL POWER/COAL-FIRED POWER

- The Design Research of 50 MVar Distributed Synchronous Compensator's Lubricating Oil System *HUANG Guowei, XUE Changkui, LI Yong*(13)
 Application Research of Electromagnetic Core Imperfection Detection Test *CHEN Zhan, YU Hongbin, LIU Hang, et al*(17)
 Development Course and Experience of DEC Heavy Duty Gas Turbine *LI Jianhua, HU Weiwei, XU Bo*(22)
 The Comparative Study of Natural Frequency Experiment and Calculation Analysis for Tube Bundle of Heat Exchanger *WANG Bo, MO Kun, LIU Biao, et al*(26)
 Accuracy Analysis and Improvement Measures of Gas Turbine Air Temperature Measurement *WU Zhifang*(30)
 Innovation and Development of Technologies for Advanced and High-efficient Ultra-supercritical Coal-fired Boiler in China *LIU Yugang, LIU Yinhe, MO Chunhong, et al*(34)

TURBINE

- The Operation Strategy of Supercritical Reheating Double Extracting Back-pressure Turbine *LUO Fang, SONG Fengqiang, HOU Mingjun, et al*(40)
 Effect of Guide Structure on Aerodynamic Performance of Exhaust Hood in Steam Turbine *PENG Guowei, HUANG Yuanong*(45)
 Research on Multi-axis N/C Machining Technology of Open-integrated Impeller *WU Zhongjing, ZHANG Chang, IAO Jie, et al*(49)
 Analysis of Vibration Characteristics of A Single Support High Power Back-pressure Unit *CAO Han, ZHAO Xianbo, I Naibin, et al*(55)

WIND POWER

- Research on Acquiring Experimental Data Acquisition System for Wind Farms *XU Fuxia, II Yuxia, CHEN Feng*(58)
 Application and Discussion of TRIZ Theory in Improvement of Yaw System of Wind Turbine *SUN Zhong e, SU Ningjie, YANG Xiaolin*(61)

HYDRO POWER

- Analysis and Research on Guide Vane Water Leakage in Large Francis Hydro-turbine Unit *SONG Min, II Haoliang, ZHANG Hong*(65)
 Optimum Design of Upper Cavity Pressure of the Runner of a Francis Turbine *HUANG Shihai, ZENG Xin, II Haoliang, et al*(70)
 Research on Flat-pressing Mode of Upper and Lower Cavities of Pump-turbine Runner *II U Long, II Haoliang, HUANG Shihai, et al*(73)

MISCELLANEOUS

- Survey of Alarm Correlation Analysis for Communication Networks Based on Machine Learning *ANG Hong, ZHOU Honglin*(77)
 Application Research of Honest Risk Prevention and Control In Post Work Flow *JANG Lina, CHEN Jian, ZHAO Xiaobo, et al*(85)
 NEWS IN BRIEF (21)(33)(44)(60)(88)

EDITORIAL BOARD

Chairman: WANG Weimin

Vice Chairmen: WANG Zheng, YANG Yong

Members: MA Qingtian, WANG Xiaoliang, WANG Yu, WANG Jianlu, WANG Zheng yuan, FANG Yu, DENG Zhongyong, LE Jinsong, SHI Qinghua, GUANG Haijie, LIU Shihong, LIU Taisheng, ZHANG Qide, ZHANG Guorong, ZOU Jie, HE Wei, CHEN Wenxue, CHEN Jiefu, YANG Wuyong, YANG Yaowu, YANG Huachun, MIN Zesheng, WU Jiandong, ZHAO Yongzhi, ZHAO Shiquan, HOU Xiaoquan, HE Jianhua, ZHONG Jie, GUO Yan, TANG Hongju, XIE Guangyou, ZENG Mingfu, LAI Chengyi, PAN Qiangang, HUO Suoshan

Chief Secretary: YANG Yong

Sponsor: Dongfang Electric Corporation

Chief Editor: WANG Weimin

Vice Chief Editors: WANG Zheng, YANG Yong

Executive Editor: WANG Weimin

English Editor: WANG Weimin

Edited and Published by:

Editorial Department of Dongfang Electric Review
 No. 18 Xi Xin Avenue, Gao Xin Xi District, Chengdu,
 Sichuan, P. R. China

Postal Code: 611731

Tel: 028-87898262 87898263 **Fax:** 028-87898267

E-mail: dfdqpl@dongfang.com

Overseas Distribution by:

China National Publishing Industry Trading Corporation
 (P. O. Box 782, Beijing, P. R. C.)

1	1	2	2	3	4
	1.			611731 2.	150001
	3.			511455 4.	611731

102.410 Hz 77.349 Hz

74.711 Hz

2

1%

TL364

A

1001-9006 2021 01-0001-04

Modal Test and Simulation of Nine-tube Prototype of Liquid Sodium Heat Exchanger

PENG Fan¹, WANG Liwen¹, ZHENG Wu², ZHANG Shengyu², LIAO Baifeng³, CAO Xuefan⁴

(1. DEC Academy of Science and Technology Co., Ltd., 611731, Chengdu, China; 2. Harbin Institute of Technology, 150001, Harbin, China;

3. Dongfang Electric (Guangzhou) Heavy Machinery Co., Ltd., 511455, Guangzhou, China;

4. Dongfang Electric Co., Ltd., 611731, Chengdu, China)

Abstract: The dynamic characteristics of the heat exchanger are closely related to the safety performance and operating efficiency of the nuclear power plant. In order to assess the fluid-induced structural vibration, a modal test through a nine-tube prototype is conducted to obtain the natural vibration characteristics of the heat exchange tube in the air and water environment. The fundamental frequencies of the heat exchange tubes in the air and water environment are 102.410 Hz and 77.349 Hz respectively, and the correction value of the fundamental frequency of the heat exchange tubes in the liquid sodium derived by the above experiment data is 74.711 Hz; finally, the high reliability of the test results is verified by the finite element analysis, the relative error of the first two natural frequency results of the test and simulation calculations is within 1%, and the simulation analysis results are important references in the structural design and optimization stage.

Key words: liquid sodium heat exchanger; heat exchange tube; modal test; simulation

1

2

3

4-5

2020-06-01

2017YFF0107300

1995 - 2019

1

1.1

1				
1	48	AD	24	24 102.4 kHz
2	32	1 mV m ⁻¹ s ⁻² 2 ~ 10 000 Hz		500 g 1.2 g
3	1	0.199 mV N ⁻¹ 40 kHz		25 000 N ±2%

1.3

2

9

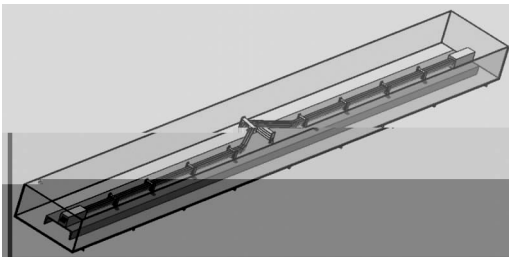
10

1

48

1

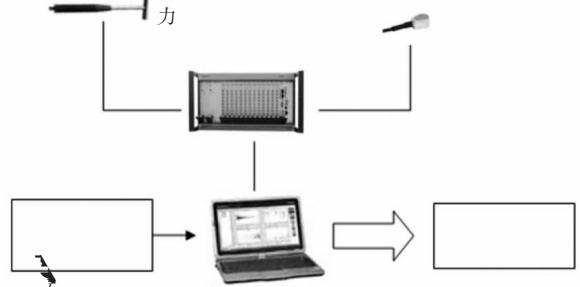
10



1

1.2

3 3
1 4 12



2



3

3

4

16

5

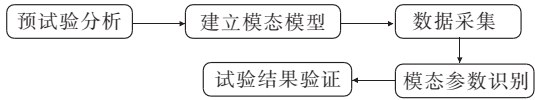
3

5

32

1

2



4

2

2.1

5

2

1 102.410 Hz 77.349

Hz

2

	/Hz	/%	/Hz	/%
1	102.410	2.012	77.349	6.886
2	115.476	2.107	86.364	4.836
3	125.120	3.159	113.612	3.623
4	131.726	1.386	125.582	2.143
5	141.214	4.111	131.533	2.836
6	150.679	2.051	142.661	1.656
7	160.724	1.107	157.146	1.614
8	176.665	1.620	166.496	1.465
9	184.608	1.768	173.697	1.415
10	189.679	0.775	179.295	1.678

2.2

1 C_M 2

6

$$f \sqrt{\frac{m_t}{EI}} = f \sqrt{\frac{m_t + m_i + m_0}{EI}} \quad 1$$

$$f \sqrt{\frac{m_t}{EI}} = f \sqrt{\frac{m_t + m_{iNa} + m_{0Na}}{E_T I}} \quad 2$$

$$m = m_t + m_i +$$

m_0

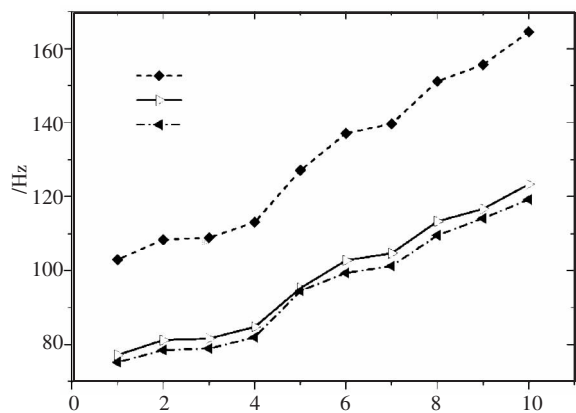
m_t

kg/m m_i

	Hz	Hz	%	Hz	Hz	%	Hz	Hz	%
1	102.410	102.940	0.51	77.349	77.159	0.25	74.711	75.180	0.62
2	-	108.320	-	-	81.188	-	-	78.503	-
3	-	108.860	-	-	81.596	-	-	78.897	-
4	115.476	113.060	2.14	86.364	84.741	1.92	83.365	81.938	1.74
5	125.120	127.050	1.52	-	95.229	-	-	94.488	-
6	131.726	137.060	3.89	-	102.730	-	-	99.332	-
7	141.214	139.650	1.12	-	104.670	-	-	101.210	-
8	150.679	151.140	0.31	113.612	113.280	0.29	108.779	109.530	0.69
9	160.724	155.630	3.27	-	116.650	-	-	114.080	-
10	-	164.500	-	125.582	123.300	1.85	121.441	119.220	1.86

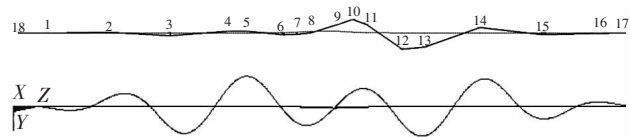
$$= | \frac{\text{Hz}_1 - \text{Hz}_2}{\text{Hz}_1} | \times 100\%$$

6

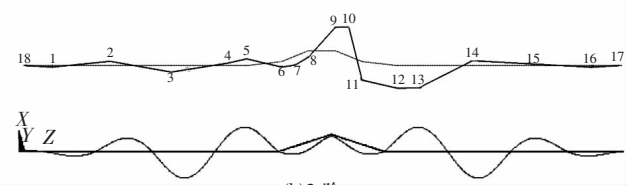


6

7



(a) 1阶



(b) 2阶

7

2

3

1

102.410 Hz

77.349 Hz

74.711 Hz

2

2

1%

8

X53

A

1001-9006 2021 01-0005-04

Analysis of Soil Remediation Technology

TIAN Jian, WU Jiahua, HU Chunyun, XIE Fei, ZHANG Yuan

(DEC Academy of Science and Technology Co., Ltd., 611731, Chengdu, China)

Abstract: This article mainly introduces the current situation of soil pollution and the market capacity of soil remediation in China, summarizes the main existing soil remediation technologies at home and abroad, and evaluates and compares these methods. The future development of soil remediation is also prospected in this article.

Key words: soil pollution; soil remediation; heavy metals; organic pollutants

2

1

2014

16.1%

2.1

2.1.1

/

Solidification/Stabilization S/

¹ 2017

S

151.45

2018

S/S

²

S/S

270

2024

860

S/S

2020-06-22

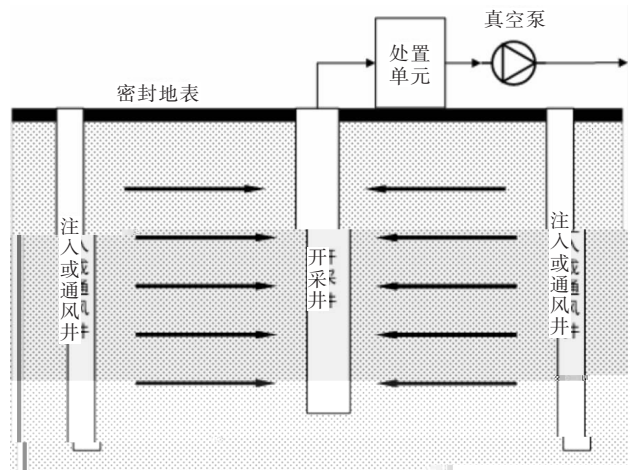
1993 - 2019

S/S

MPE

3

S/S



2.1.2

/ S/S
/
/
/
3
/
/

PAHs

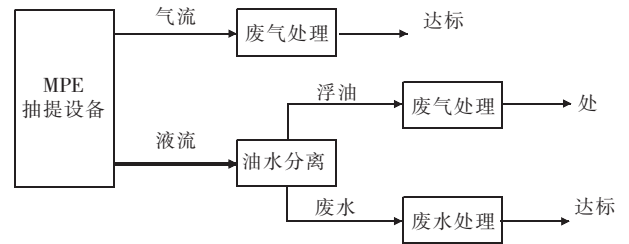
/

2

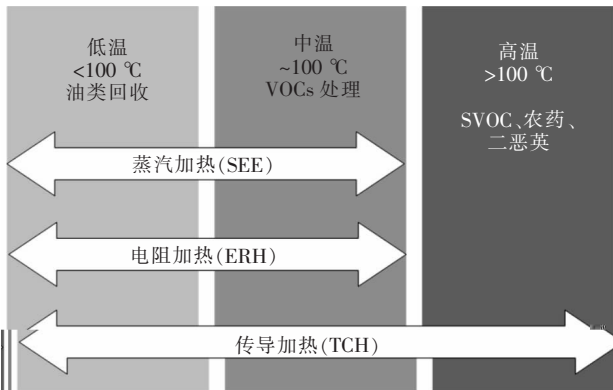
ERH

TCH

SEE 3



1



3 MPE

SVE/MPE

1

2.1.3

/

Soil Vapor Extraction SVE

/

SVE

2

Multi-Phase Extraction MPE

2.2

2.2.1

2.3.2

7

5

2.2.2

2.3.3

2.4

+

SO₂ H₂S

Fe⁰

2.5

2.2.3

6

SVE

1

3

2.3

2.3.1

Al³⁺

Al

Al

pH

Al

1

		/ . t ⁻¹
/	/	200 ~ 800
/	/	400 ~ 500
/	SVE MPE	SVE 100 ~ 300 MPE SVE 400 ~ 500
		150 ~ 500
	/	300 ~ 1 500
	/	500 ~ 1 500 500 ~ 1 500 400 ~ 1 900
		100 ~ 500
		300 ~ 400
		100 ~ 200

J . 2019 5 245

2

4

1 . J .

2019 1 47 - 50

2 . /

	1	2	2	
1.		611731	2.	611731

1.0 ~ 1.5 V
1

2

1 000

TM911.4

A

1001-9006 2021 01-0009-04

Study on the Effect of Cracks in Catalyst Layer on the Durability of PEMFC Membrane Electrode Assembly

XIE Guangyou¹, ZHU Leifeng², LI Ting²

1. Dongfang Electric (Chengdu) Hydrogen Fuel Cell Technology Co. , Ltd. , 611731, Chengdu, China;

2. Sichuan Key Laboratory of Long-life Fuel Cells, 611731, Chengdu, China)

Abstract: Cracks are easily generated in catalyst layer due to the thermal stress between surface and inside during catalyst ink coated on membranes. Catalyst layer containing cracks in different degree of severity are prepared in this paper. The effect of cracks on the durability of membrane electrode assembly is studied by the accelerated durability test. After 1 000 cycles of potential scanning between 1.0 ~ 1.5 V, compared with CCM containing no cracks, the decay rate of the performance electrode with networked cracks increases by two times, and the decay rate of ECSA is double.

Key words: PEMFC membrane electrode assembly; catalyst layer; cracks; durability

Membrane Fuel Cell PEMFC
Proton Exchange
95%¹
catalyst coated
membrane CCM
gas diffusion
electrode GDE ②
decal
21
process⁵
-

2

3-4

①

2020 - 09 - 28

1983 - 2011

6

X FE-SEM

7

TESCAN VEGA3

2

3

3

2.1

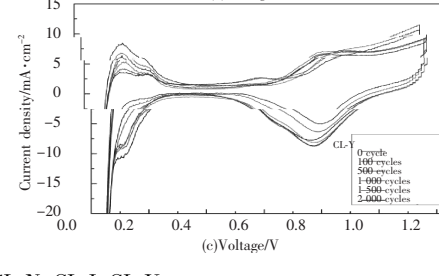
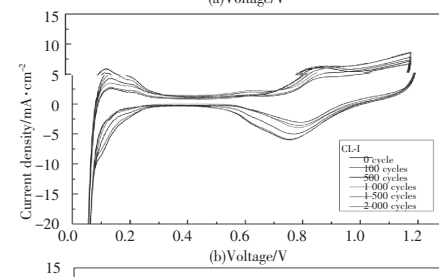
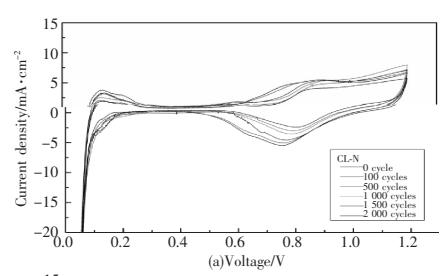
1 000 2 000 CL-N
CL-I CL-Y 0.1 1.0 A/cm²
1
0.1 1.0 A/cm²
1.0 A/cm² 2 000
CL-N I
CL-I 1 Y
CL-Y 2
1 CL-N CL-I CL-Y

Sample	CL-N		CL-I		CL-Y		
Cycle number	1 000	2 000	1 000	2 000	1 000	2 000	
Degradation Rate/%	0.1 A/cm ²	3.48	4.97	3.72	5.46	13.10	21.36
	1.0 A/cm ²	13.57	25.27	17.99	52.67	23.72	>70

2.3

CL-N CL-I
CL-Y 3 *ECSA*

ESCA 4



4 CL-N CL-I CL-Y

CL-N
100 1 000 2 000
ECSA
3 *ECSA*
2
1 000
CL-N I
CL-I *ECSA* 77.7% Y
CL-Y
ECSA

Sample	CL-N	CL-I	CL-Y
<i>ECSA</i> Degradation Rate /%	100 cycles 4.93	16.79	15.84
	1 000 cycles 25.62	45.54	53.91
	2 000 cycles 46.31	52.28	65.02

3

2
1

1 M
2003
2 M 2010
3 Frisk JW Hicks MT Atanaski RT et al. MEA Component Durability R . Office of Scientific & Technical Information Technical Reports 2004
4 Li X Sabir I. Review of bipolar plates in PEM fuel cells Flow-field design J . International Journal of Hydrogen Energy 2004 30 4 359 – 371

50 MVar

618000

50 MVar

TM621

A

1001-9006 2021 01-0013-04

The Design Research of 50 MVar Distributed Synchronous Compensator's Lubricating Oil System

HUANG Guowei, XUE Changkui, LI Yong

(Dongfang Electric Machinery Co., Ltd., 618000, Deyang, Sichuan, China)

Abstract: According to the layout environment and safe operation requirements of the 50MVar distributed synchronous compensator, this paper researches the design of synchronous compensator's lubricating oil system and calculates the tank capacity of the lubricating oil system, the flow and pressure of the lubricating oil pump, and the heat exchange area of the oil cooler, which provides a theoretical basis for the selection of system equipment.

Key words: distributed synchronous compensator; lubricating oil system; flow and pressure of the lubricating oil pump; tank capacity; exchange area

300 MVar

1

50 MVar

2

1

1 1

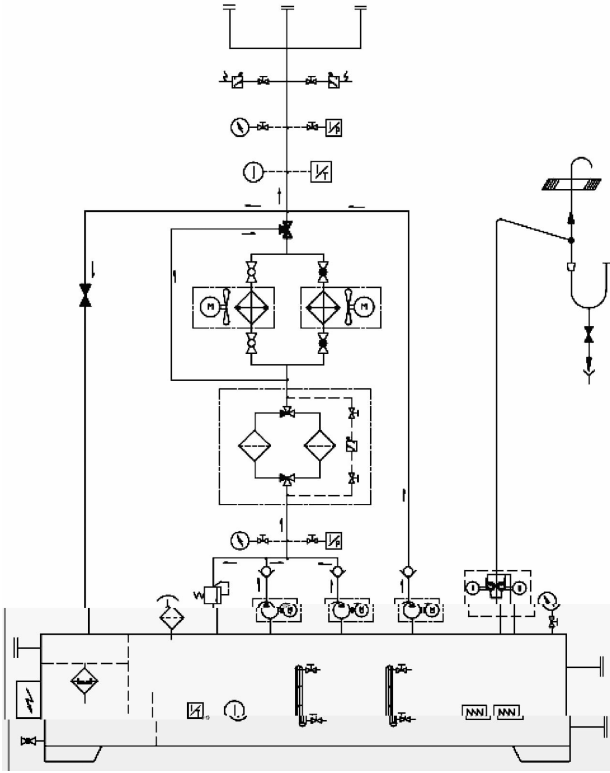
1

2020-06-22

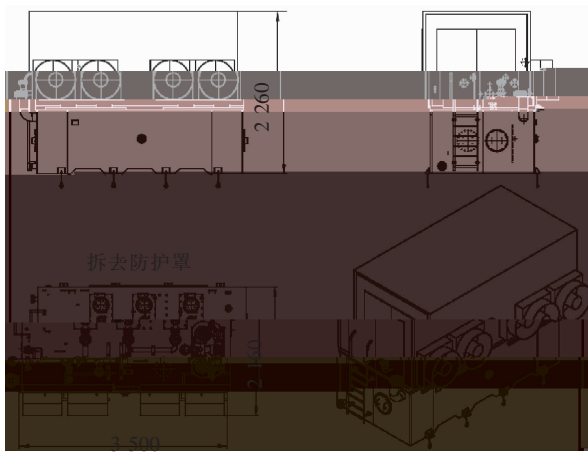
1987-2010

1987-2012

2

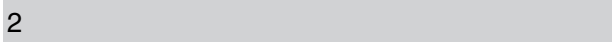


1



2

1



2

1

	kW	P	68
	kW	H	20
	min	t	40
	°C	T_0	30
	°C	T_1	40
	°C	T_2	55
	°C	T_3	75
	MPa	P_1	0.1

2.1

32#

$$Q = \frac{P}{C \Delta T_1} \quad 1$$

$$886 \text{ kg/m}^3 \quad C$$

$$1.92 \text{ kJ/kg}^\circ\text{C} \quad \Delta T_1$$

$$\Delta T_1 = T_2 - T_1 \text{ }^\circ\text{C}$$

$$159 \text{ L/min}$$

$$5 \text{ r/min}$$

$$160 \text{ L/min}$$

2.2

2

2

			90°	
d/mm	l/m			
50	30	6	1	6
32	15	4	0	0

2.2.1

$$Re = \frac{vd}{\nu} = \frac{1.274Q}{d} \times 10^4 \quad 2$$

$$Q \quad 160 \text{ L/min}$$

$$80 \text{ L/min} \quad 0.32 \text{ St}$$

$$Re_1 = 2 \ 123$$

$$Re_1 = 1\ 659$$

$$Re_L = 2\ 320$$

1

2.2.2

$$\Delta P_L = \frac{l}{d} \times v$$

$$C \quad \text{kJ/kg } ^\circ\text{C} \quad G$$

$$G = Q / A_e \quad \text{kg/m}^2 \cdot \text{s} \quad Q$$

$$\text{m}^3/\text{h} \quad St \quad St = j/Pr^{2/3} \quad j$$

$$Re \quad j-Re$$

$$Pr \quad Pr = \mu C / \quad Re$$

$$Re = GD_e / \mu g \quad \mu \quad 1.88 \times$$

$$10^{-5} \text{Pa} \cdot \text{s} \quad 2.83 \times 10^{-3} \text{Pa} \cdot \text{s}$$

$$0.025 \text{W/K} \cdot \text{m} \quad 0.15 \text{W/K} \cdot \text{m}$$

$$\text{kg/m}^3 \quad g \quad 9.8 \text{m/s}^2$$

$$1 = 12.78 \text{kJ/m}^2$$

$$\text{h } ^\circ\text{C} \quad 2 = 415 \text{kJ/m}^2 \cdot \text{h } ^\circ\text{C}$$

4.3.2

$$= 1 - \frac{F_{o2}}{F_o} \quad 1 - \quad r \quad 11$$

$$r \quad r = \tanh \quad h \quad \text{ml} \quad / \text{ml} \quad m$$

$$m = \sqrt{2 / \quad m} \quad l$$

$$l = h_1 \quad l = h_2 / 2 \quad m$$

$$735 \text{kJ/m}^2 \cdot \text{h } ^\circ\text{C}$$

$$1 = 0.772$$

$$2 = 0.978$$

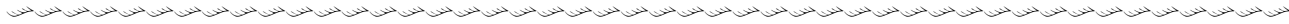
4.3.3

$$K_1 = \frac{1}{\frac{1}{1} + \frac{1}{2} \cdot \frac{F_1}{F_2}} \quad 12$$

$$K_2 = \frac{1}{\frac{1}{2} + \frac{1}{1} \cdot \frac{F_2}{F_1}} \quad 13$$

$$K_1 = 20.75 \text{W/m}^2 \cdot ^\circ\text{C} \quad K_2 = 103.6 \text{W/}$$

$\text{m}^2 \cdot ^\circ\text{C}$



12

5 Kocha SS. Handbook of Fuel Cell Fundamentals Technology and Application M . Vielstich W Lamm A Gasteiger H A. Editors Vol. 3 John Wiley & Sons New York 2003

6 Tsushima S Hirai S. An overview of cracks and interfacial voids in membrane electrode assemblies in polymer electrolyte fuel cells

4.4.4

$$\Delta t_m = \frac{\Delta t_1 - \Delta t_2}{\ln \frac{\Delta t_1}{\Delta t_2}} \quad 14$$

$$\Delta t_1 \quad 15 ^\circ\text{C} \quad \Delta t_2$$

$$7 ^\circ\text{C} \quad \Delta t_m =$$

$$10.5 ^\circ\text{C}$$

4.4.5

$$F = \frac{P}{K \Delta t_m} \quad 15$$

$$312 \text{m}^2$$

$$62.5 \text{m}^2 \quad 2$$

30% ~ 50%

2

5

1 . M . .

2004

2 .300 MVar J .

2018 32 3 70 -72

3 . M . 1984

4 .

J . 1972 4 27 -33

J . Journal of Thermal Science and Technology 2015 10 1 JTST0002

7 Banan R Zu J Bazylak A. Humidity and Temperature Cycling Effects on Cracks and Delaminations in PEMFCs J . Fuel Cells 2015 15 2 327 -336

EL-CID

618000

EL-CID 4%
EL-CID
EL-CID EL-CID
EL-CID
TM31 A 1001-9006 2021 01-0017-05

Application Research of Electromagnetic Core Imperfection Detection Test

CHEN Zhan, YU Hongbin, LIU Hang, LIU Xiao

(Dongfang Electric Machinery Co., Ltd., 618000, Deyang, Sichuan, China)

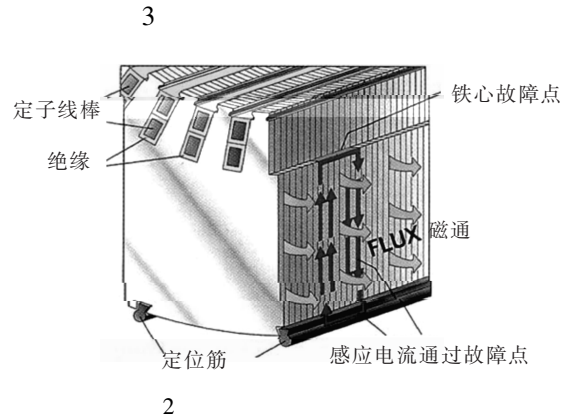
Abstract: To inspect the stator core assembly of generator, it is imperative to conduct test for core in manufacture and power plant. At present, for stator core, we preferentially adopt routine test at home, but such routine core loss test requires equipments with large capacity and complex test circuit, which is less economical and inefficent. By contrast, EL-CID core test merely applies 4% of rated flux to diagnose the tested object, what's more, it equips with the power source with comparate

1.4 T

1.0 T

90°

QUAD



2 EL-CID

2.1

EL-CID

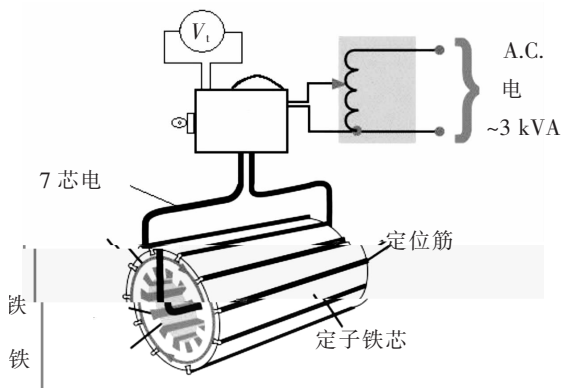
1

4%

Chattock

4%

Chattock



1 EL-CID

2

2.2

GB/T20835-2016

C EL-CID

100 mA

Phase

4%

100 mA

5 K ~ 10 K

3

EL-CID

GB/T20835-2016

1

3.1

1

EL-CID

4

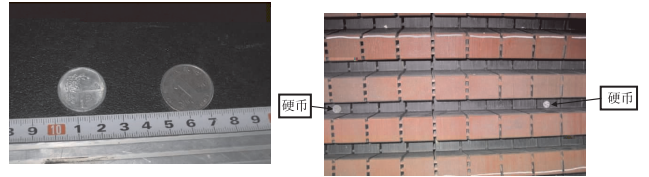
1

- 3.1.1
- 3.1.2
- 3.1.3
- 3.1.4 "L"

- 3.1.5 "U"
- 3.1.6 "U"

- 3.2.1
- 3.2.2
- 3.2.3

3.3 EL-CID



3

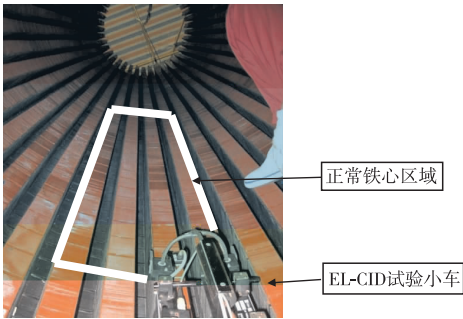
6



7

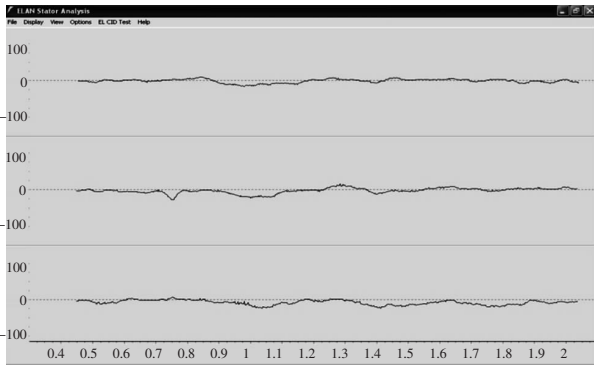
16 cm D2

7 EL-CID



4

5

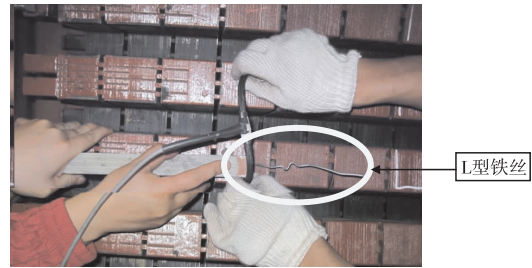


5

100 mA

4 "L"

8



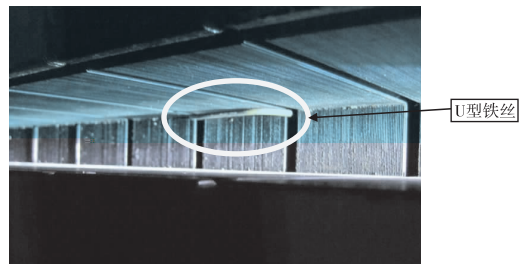
8

L

EL-CID

5 "U"

9



9

U

EL-CID

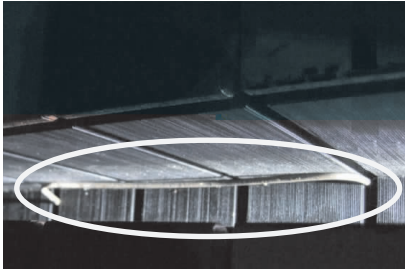
EL-CID

2

6 EL-CID

6 “U”

10



U型铁

1

2

4.2 EL-CID EL-CID
 1 4%

2

100 mA

1 GB/T20835 - 2016
 2016

S .



660 MW

2021 2 5

660 MW

— 2

75% 50%

8.9 9.3 17.4

4.02

"

"

660 MW

2

1 000 MW

"

—

—

—

"

来源:东方电气网

	1	2	1
1.	611731	2.	618000

TK474.8

B

1001-9006 2021 01-0022-04

Development Course and Experience of DEC Heavy Duty Gas Turbine

LI Jianhua¹, HU Weiwei², XU Bo¹

(1. Dongfang Electric Co., Ltd., 611731, Chengdu, China; 2. Dongfang Turbine Co., Ltd., 618000, Deyang, Sichuan, China)

Abstract: This paper reviews the process from the technology introduction of gas turbine industry, the formation of manufacturing localization capacity, and the integration of innovation from the beginning to the final success, focusing on the practice and features of Dongfang Electric's independent innovation, so as to provide a reference for the innovation work of the industry and enterprises.

Key words: gas turbine; natural gas power generation; technology introduction; integration and innovation

1

2002

GE
MHI

SIEMENS

2002

2020 - 10 - 12

1972 - 1994

1972 - 1992

1982 - 2008

1

1.	1		1
	2		2
	3		
	4		
	5		
	6		
	7		
	8		
2.	1		1
	2	/	2
3.	1		1
	2		2
4.	1		
	2		
	3		
5.			
6.			

			2000	2008	
1	2008	2002 ~			86 000
		2001 10			
	2001 2194	" "			/
	24	56			
		GE			
		Siemens			
Ansaldo			4 067	525	
			1 500		
			FAI		

2008

57%

59%

M701F4

M701F4

GE

F

1

2 M701F4

2

/kW

/%

kJ/kW h

GE	9FA	390 800	56.7	6 350
----	-----	---------	------	-------

Siemens	SGT5-4000F	407 000	57.7	6 239
---------	------------	---------	------	-------

MHI	M701F4	450 000	59.0	6 120
-----	--------	---------	------	-------

3

2. 2

4

5

2008

2002

2009

2

2008 ~

2014

2014

TBC

3

2. 1

3. 1

GE

2014

2007

F J

Gas Turbine World 2005

MHI M701F4

40%

M701F4


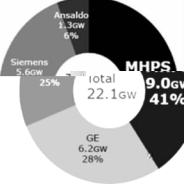
2 ISO

M701F4 2008

2018 GE

100 MW

1

Market Share No.1 + 100 MW and above

MHPS has achieved a major milestone in the global Power Generation sector, securing 2018 market share leadership in global orders. Based on data compiled by McCoy Reports (Technology Owner basis), MHPS' heavy duty turbines captured 41% global market share for heavy duty gas turbines in the category of 100 MW and above. MHPS market leadership was driven by the J-Series gas turbine.

"Mitsubishi wins on new technology."
- Reuter

"The effect of integrating the merits of Mitsubishi and Hitachi is fruited in years"
- The Nikkei

1 2018 MHPS 100 MW

3.2

F 50 MW

1	2	2	2	1	2
1.	611731 2.			611731	

3

2 2%

TK172

A

1001-9006 2021 01-0026-04

The Comparative Study of Natural Frequency Experiment and Calculation Analysis for Tube Bundle of Heat Exchanger

*WANG Bo*¹, *MO Kun*², *LIU Biao*², *WANG Liwen*², *CAO Xuefan*¹, *FENG Lin*²

(1. Dongfang Electric Co., Ltd., 611731, Chengdu, China; 2. DEC Academy of Science and Technology Co., Ltd., 611731, Chengdu, China)

Abstract: The vibration analysis is very important for the safety evaluation of heat exchanger. The key in vibration analysis is the acquisition of system modal characteristics. In order to effectively evaluate the safety and reliability of the once-through heat exchanger, a series of modal tests of heat exchange tubes are carried out on feature unit. On this basis, the modal simulation and theoretical calculation of heat exchange tube are carried out. The analysis show that the natural frequency results obtained by the three methods are in good agreement with each other, and the relative error of the natural frequency between experimental results and the simulation results (the first 2 orders) is within 2%. The validity of the analysis results is confirmed.

2020 - 07 - 19

1986 - 2013

1

1.1

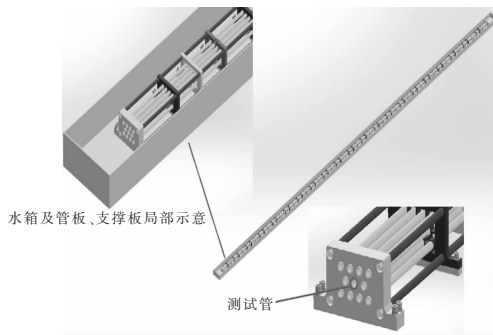
1 11

21 3

4

4

21



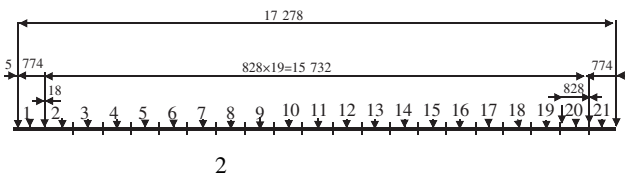
1

1.2

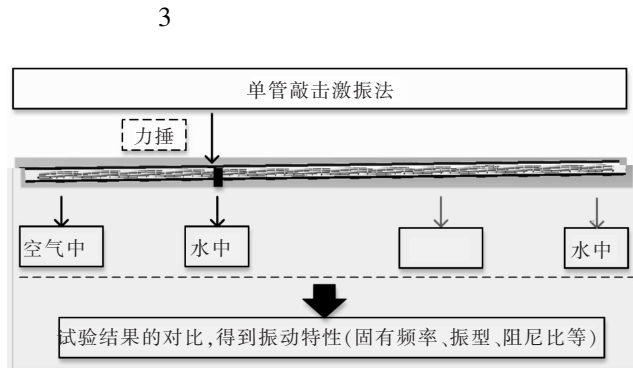
21

2

1.3



2



3

3

7

5

2

2.1

1

5

5

0.2

1

	/Hz	/%	/Hz	/%
1	54.317	1.196	55.687	3.999
2	55.111	2.697	56.673	4.490
3	57.815	1.847	59.190	4.454
4	60.136	2.297	61.724	4.649
5	62.603	1.452	64.485	4.143
6	66.858	1.956	71.583	6.261
7	70.447	2.625	73.763	6.510
8	75.838	2.001	79.545	5.430
9	80.454	1.611	82.693	4.775
10	84.816	2.270	87.373	3.416

1

54.317 Hz

1

E S

55.687 Hz

2.2

2

1

47.227 Hz

1

48.013 Hz

2

	/Hz	/%	/Hz	/%
1	47.227	1.802	48.013	5.459
2	48.706	3.597	49.027	6.138
3	49.844	2.453	50.695	5.670
4	52.492	2.489	53.754	7.008
5	54.072	2.197	54.665	5.518
6	57.947	2.917	60.028	6.698
7	61.397	3.751	62.149	5.172
8	65.492	3.492	68.214	6.952
9	69.278	3.019	71.980	6.217
10	74.319	2.886	74.788	6.453

3

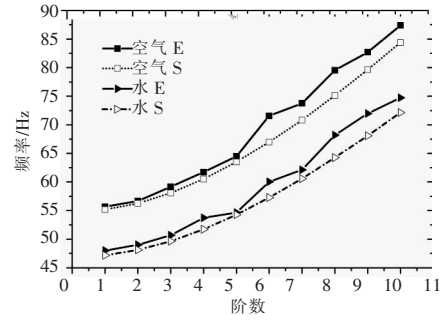
3.1

4



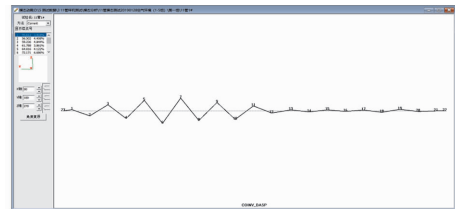
4

5

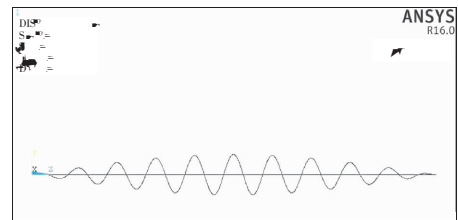


5

6 7

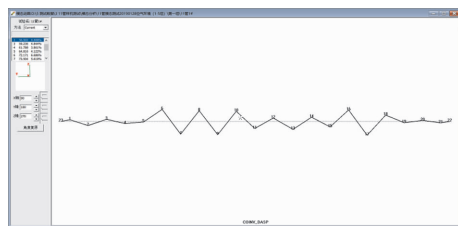


a

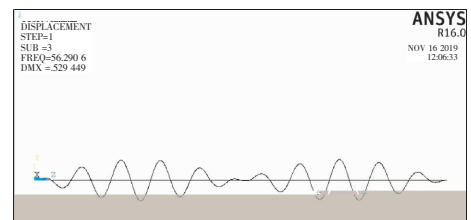


b

6



a



b

7

4

1

54.317 Hz

47.227 Hz

3.2

GBT151 2014

C

2

1

$$f_n = 35.3 \sqrt{\frac{E(d_0^4 - d_i^4)}{ml^4}} \quad 1$$

f_n Hz

rad E MPa d_0

m d_i m m

kg/m l m

3

3

3

	Hz	1 %	2 %	Hz	1 %	2 %
1	55.122	0.91	0.11	47.400	1.77%	-0.47
2	56.236	0.70	0.08	48.357	1.88	-0.48

1

2

3

2

1%

2

2%

3

TK477

B

1001-9006 2021 01-0030-04

Accuracy Analysis and Improvement Measures of Gas Turbine Air Temperature Measurement

WU Zhifang

(Dongfang Electric Autocontrol Engineering Co., Ltd., 618000, Deyang, Sichuan, China)

Abstract: The power of gas turbine has a great relationship with air temperature. When the control system controls the power of gas turbine, the measurement accuracy of input air temperature signal must be accurate enough to realize the accurate control of gas turbine power. In this paper, combined with a control system example, the accuracy of air temperature signal measurement loop is analyzed, and the improvement method to improve the measurement accuracy is given. By improving the measurement accuracy of the air temperature signal, the power of the gas turbine can be accurately controlled, and the efficiency of the gas turbine can be improved, which will bring higher economic benefits to the gas turbine power plant.

Key words: air temperature; measurement accuracy; improvement

P T P
3 ①

②

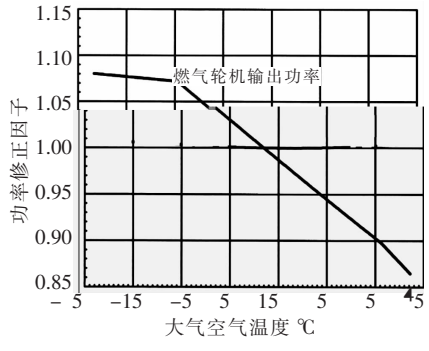
1

1.1

T

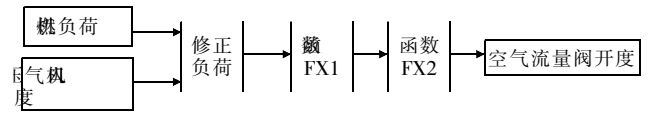
2020 - 08 - 31

1982 - 2004



1

2.2



3

2



TC

0.4

400 ppm/deg C

A/D

3

RTD

6

AI	4 ~ 20 mA	AO	4 ~ 20 mA	AI	4 ~ 20 mA
DI		DO	RTD	RTD	2
			2	AI	

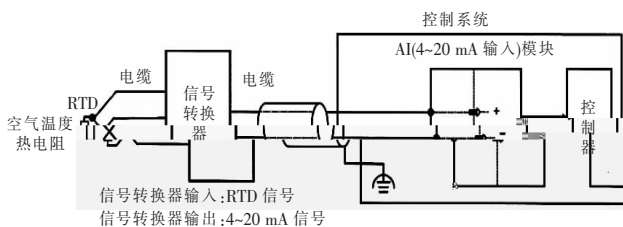
	RTD	AI 4 ~ 20 mA
1	-40 ~ 60 deg C	4 ~ 20 mA
2	± 0.1% FSD	± 0.1% FSD
3	± 400 ppm/deg C	± 100 ppm/deg C

5

RTD

4 ~ 20 mA

AI 4 ~ 20 mA



5 RTD

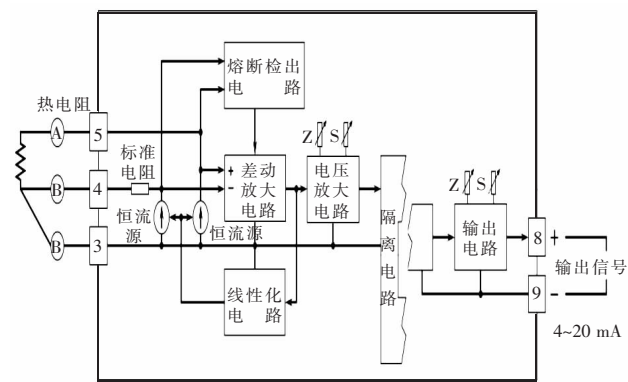
4 ~ 20 mA

3

4 ~ 20 mA

6

3



6

AI 4 ~ 20mA

3

1	-200 ~ 660 deg C	-200 ~ 660 deg C
2	± 0.2 %	± 0.01 %
3	± 0.2 %	± 0.04 %
4	± 150 ppm/deg C	± 100 ppm/deg C

$$\% = 0.2\% \times 860/100 + 0.2\%$$

$$\% = \quad \times 860 / 100 + 0.015\% \times 15 \text{ deg} = 2.145\%$$

$$+ \quad \times \quad 15 \text{ deg C} \quad \% = 0.01\% \times 860/100 + 0.04\% +$$

$$0.01\% \times 15 \text{ deg} = 0.276\%$$

0.4

+ AI 4 ~ 20 mA

5

6 AI 4 ~ 20 mA

AI

$$\text{AI} \quad \% = 0.1\% + 0.01\% \times 15 \text{ deg}$$

$$= 0.25\%$$

RTD

% =

+ AI 4 ~ 20 mA

$$\sqrt{\text{AI}^2 + \text{AI}^2} + \text{AI 4 ~ 20 mA}$$

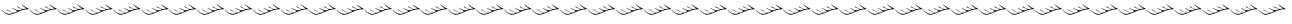
% =

$$\sqrt{0.25 \times 0.25 + 0.276 \times 0.276} \% = 0.372\%$$

$$\text{deg C} = 60 + 40 \times 0.372\% = 0.372$$

deg C 0.372

2002 310 - 312



2021 1 30

5

10

1 828 mm

MPa/538 °C/566 °C

2

2000

2004

2	620 °C
Π	
+	

620 °C	600 °C
3	
OPCC	
P92	
150 mm	

620 °C	600 °C
1	
Π	
OPCC	

30 °C ~ 50 °C ⁷
2
3

23	
T92	623 °C
649 °C	26 °C
1#	
15 °C	10 °C
	1#

623 °C	
94.64% NO _x	170 mg/Nm ³

620°C			
	2019	660 MW	40
120	1 000 MW	20	70

2

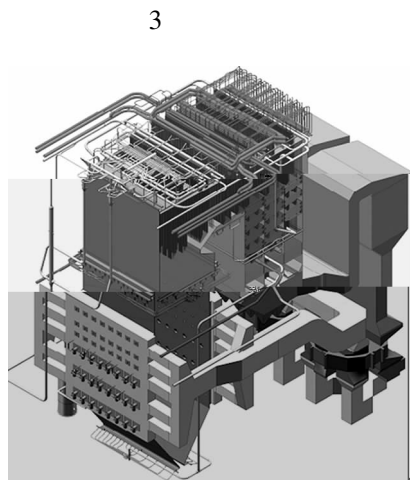
620°C
③
②
①

50 ~ 100%
 BMCR

①
②

23 - 24

4



2

		3	620 °C
		/	620 °C
		/MPa	32.5 29.4
		/°C	605 605
		/°C	623 623
		/°C	623 /
		/°C	~330 300 ~ 315
	1#	3	620 °C
620 °C		3	
660 MW	3#	4	
	2018		
		4	

2 × 660 MW	32.45 MPa/605 °C/623 °C/623 °C	Π	+
2 × 660 MW	32.45 MPa/605 °C/623 °C/623 °C	Π	
2 × 660 MW	34.65 MPa/605 °C/623 °C/623 °C		+
2 × 660 MW	32.68 MPa/605 °C/623 °C/623 °C		+
2 × 1 000 MW	33.3 MPa/605 °C/613 °C/613 °C	Π	+
2 × 1 000 MW	33.2 MPa/605 °C/623 °C/623 °C	Π	+
2 × 1 000 MW	33.5 MPa/605 °C/623 °C/623 °C	Π	
2 × 1 000 MW	36.75 MPa/620 °C/633 °C/633 °C	Π	
2 × 1 000 MW	32.45 MPa/605 °C/623 °C/623 °C		+
2 × 1 000 MW	33.2 MPa/605 °C/623 °C/623 °C	Π	+
2 × 1 000 MW	33.5 MPa/605 °C/623 °C/623 °C	Π	+
2 × 1 000 MW	33.5 MPa/605 °C/623 °C/623 °C		+
2 × 1 000 MW	33.3 MPa/605 °C/623 °C/623 °C		+
2 × 1 000 MW	32.45 MPa/605 °C/623 °C/623 °C	Π	+
2 × 1 000 MW	34.21 MPa/605 °C/613 °C/613 °C		+
2 × 1 000 MW	33.1 MPa/605 °C/623 °C/623 °C		+
2 × 1 000 MW	33.6 MPa/605 °C/623 °C/623 °C		+
2 × 1 000 MW	32.45 MPa/605 °C/623 °C/623 °C		+
1 × 1 350 MW	32.58 MPa/612 °C/631 °C/625 °C		+

3

SA-213S30432
SA-213TP310HCbN 700 °C
SA-335P92
600 °C ~ 620 °C
620 °C

G115

G115

700 °C

630 °C

23 27

700 °C

630 °C 700 °C

620 °C

5

" 3

"

620 °C

5

/	700 °C	630 °C	620 °C
/MPa	36.75	36.75	32.5
/°C	705	620	605
/°C	723	633	623
/°C	723	633	623
/°C	~ 330	~ 330	~ 330

3.1 630 °C

630 °C

S31035

G115

630 °C

23 27

S31035

G115

G115

S31035

T91

G115

3.2 700 °C

700 °C

-

Alloy617B IN740H Haynes282

GH984G²⁸⁻³⁷

GH984G

GH2984

700 °C

³⁷

-

³⁷

SMC

IN740H

IN740H

700 °C

700 °C

³⁸

M

³⁹

U

⁴⁰

4

600 °C

620 °C

630 °C

700 °C

1

J .

- 2013 32 29 1-8
2 . 1 000 MW
J . 2009 1 10-14
3 . J .
2008 30 2 1-4
4 .700 °C J .
2012 17 6 13-17
5 .700 °C J .
2013 34 8 69-75
6 Siefert J A Tanzosh J M Ramirez J E. Advances in Materials
Technology for Fossil Power Plants C //Proceedings from the 6th
International Conference 2010. Ohio ASM International 2011 1045
7 . 1 000 MW
J . 2015 29 4 26-30
8 . J .
2011 27 1 1-5
9 .
J . 2003 23 3 2363-2369
10 . J .
2000 31 1 2-11
11 .
J . 2013 64 9 3213-3219
12 .
J . 2008 28 3 334-338
13 .
R . 2005
14 .
R .
2003
15 .
R .
2002
16 .
J . 2012 45 4 101-107
17 . J . 2011
27 5 417-422
18 . II
J . 2001 32 2 1-6
19 . J .
2002 2 10-13
20 Robert Swanekamp. Return of the Supercritical Boiler J . Power
2002 146 4 32-40
21 . M .
1989
22 . M .
2007
23 .
J . 2018 51 9 73-77
24 . J .
2017 46 8 1-15
25 . 700 °C
J . 2011 31 12 960
-968
26 .700 °C Alloy 617 mod
J . 2014 34 14 2314-2318
27 .650 °C
Z .2016-5-24
28 Baker B A Gollihue R D Sanders J M et al. Coal World Energy
Security 34th International Technical Conference on Clean Coal and
Fuel Systems 2009 C . New York Curran Associates Inc
2010 399
29 Tung D C Lippold J C. Superalloys 2012 C . New Jersey John
Wiley & Sons Inc 2012 563
30 Viswanathan R Coleman K Raou. Materials for ultra - supercritical
coal-fired power plant boilers J . International Journal of Pressure
Vessels and Piping 2006 83 18 778-783
31 Natesan K Park J H. Fireside and steam side corrosion of alloys for
USC plants J . International Journal of Hydrogen Energy 2007 32
16 3689-3697
32 Bugge J Kjær S Blum R. High-efficiency coal-fired power plants
development and perspectives J . Energy 2006 31 5 1437
-1442
33 Abe F. Research and development of heat-resistant materials for
advanced USC power plants with steam temperatures of 700 °C and
above J . Engineering 2015 22 2 150-156
34 Klöwer J Husemann R U Bader M. Development of nickel alloys
based on alloy 617 for components in 700 °C power plants J .
Procedia Eng. 2013 55 3 226-231
35 Zhao S Q Xie X S Smith G D et al. Research and improvement on
structure stability and corrosion resistance of nickel-base super alloy
INCONEL alloy 740 J . Mater. Des. 2006 27 6 1120-1128
36 Liu Z D Chong Y Bao H S et al. Boiler tube for 700 °C steam
parameter thermal power generating unit and preparation method
thereof P . Chin Pat 103276251 2013
37 . GH984G 700 °C
J . 2019 55 7 893-901
38 . J .
2016 35 4 1-3
39 .
CN201110090155.5
P .2011-08-10
40 .
CN201120273092.2 P .2011-07-29

1	2	1	3	3	1
1.			618000	2.	611731
		3.			300270

TM621

A

1001-9006 2021 01-0040-05

The Operation Strategy of Supercritical Reheating Double Extracting Back-pressure Turbine

LUO Fang¹, SONG Fengqiang², HOU Mingjun¹, HU Yizhang³, WANG Yong³, GONG Chuanyao¹

(1. Dongfang Turbine Co., Ltd., 618000, Deyang, Sichuan, China; 2. Dongfang Electric Co., Ltd., 611731, Chengdu, China;

3. Huadian International Power Co., Ltd., Tianjin Development Branch, 300270, Tianjin, China)

Abstract: It is one of the important directions to promote energy saving and emission reduction promoting the heating technology of back-pressure turbine continuously. Transferring the measures increasing efficiency, such as reheating, heat regenerative system optimization, graded regulation of heating, from large thermal turbine to back-pressure turbine can improve the energy efficiency furtherly. Furthermore, the energy saving measures above-mentioned increase the complexity of the system, but also increase the difficulty of unit operation. This paper takes the supercritical reheating double extracting back-pressure steam turbine for some project as an example to analyze its operation strategy for reference of similar units.

Key words: back pressure turbine; operation; startup

1

3

4.5 MPa 1.4 MPa

350 MW

CFB

2 × 50% BMCR

4.5 MPa

5.0 MPa

1 400

1

50% BMCR

t/h

1.4 MPa

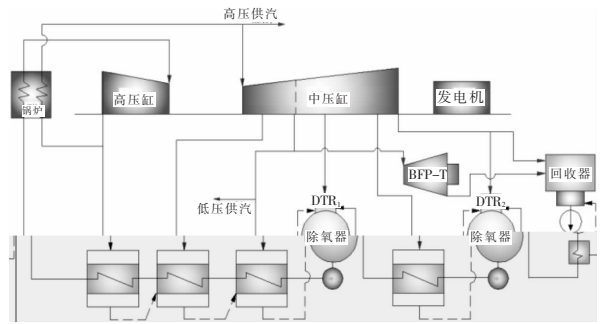
1.8 MPa

2020 - 06 - 15

CHDKJ19-01-88

1982 - 2003

600 t/h 4.5 MPa 980
 t/h 1.4 MPa 420 t/h
 4.5 MPa
 484.4 t/h 1.4 MPa 209 t/h
 3
 390 t/h 4.5 MPa
 1.4 MPa
 87% BMCR
 96% BMCR

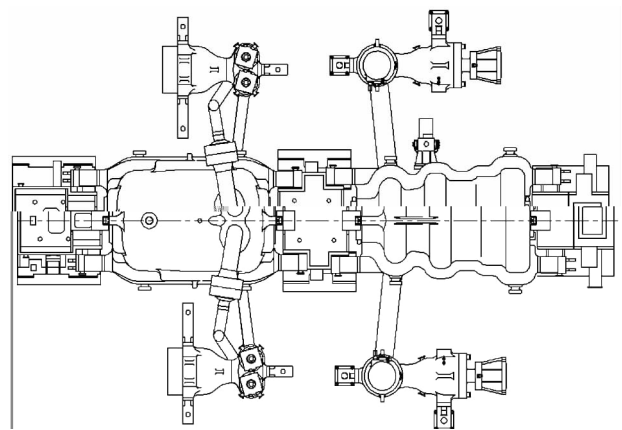


1

6

1.8 MPa

2



2

6

7

1

1.1

13

13

1

CCB157-24.2/5.0/1.8/0.15/566/453

157 MW

24.2 MPa/566 °C/453 °C

VWO

1 172 t/h

5.0 MPa 1.8 MPa

467 t/h 200 t/h

0.15 MPa

3

1

1

1

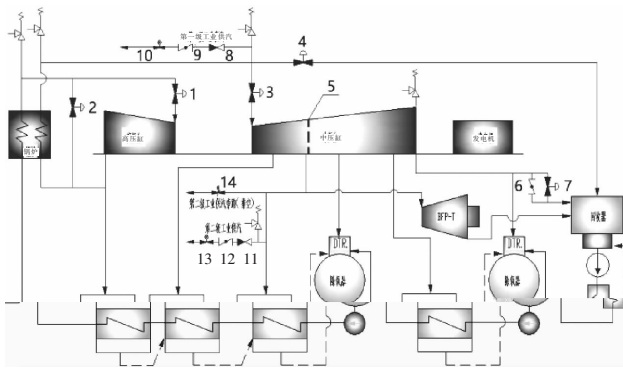
1

0.15 MPa

1.2

350 MW

3

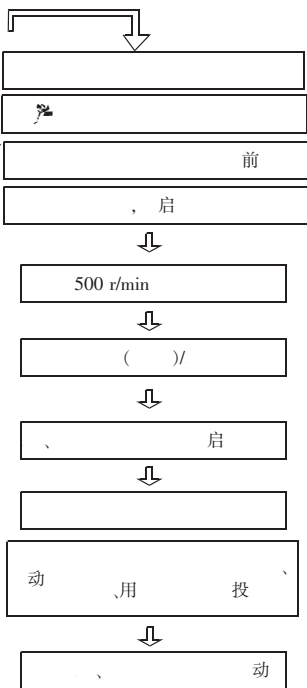
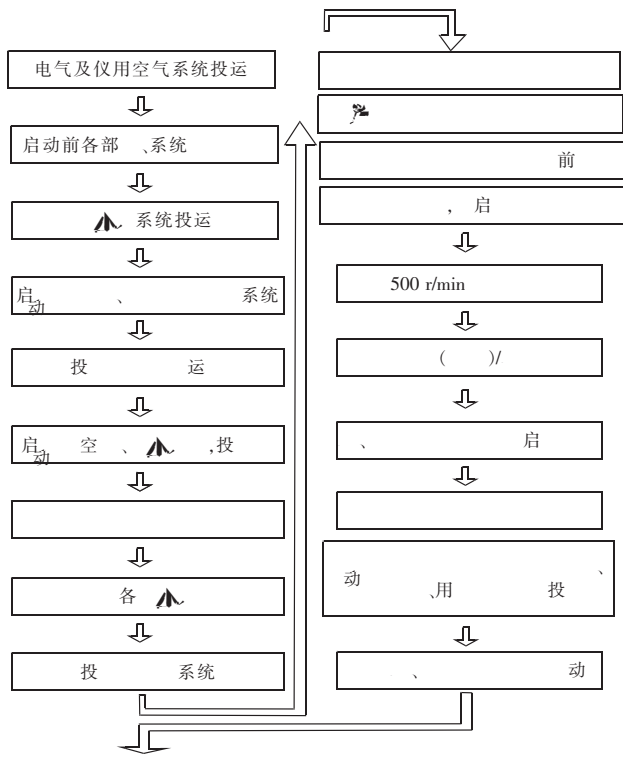


- 1
- 2
- 3
- 4
- 5
- 6
- 7
- 8
- 9
- 10
- 11
- 12
- 13
- 14

"

"

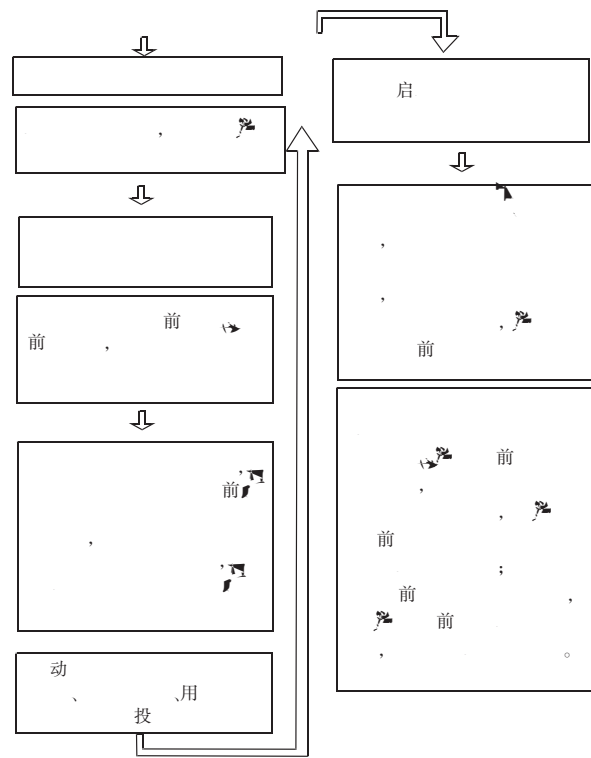
"



~ 40%

425 °C

2



4

150 g/kWh

“ ”

-
- 1 . M . 1988 3
 - 2

15°

5 600 mm

37.1%

39%

TM621

A

1001-9006 2021 01-0045-04

Effect of Guide Structure on Aerodynamic Performance of Exhaust Hood in Steam Turbine

PENG Guowei, HUANG Yuandong

(Dongfang Turbine Co. , Ltd. , 618000, Deyang, Sichuan, China)

Abstract: Based on the background of a modified steam turbine, By using numerical simulation and theoretical calculation methods to study the exhaust steam passage of the low pressure cylinder, this paper analyzes the influence of the initial diffusion angle and outer diameter of the guide ring in the exhaust steam passage of the low pressure cylinder . The results show that as the initial diffusion angle of the diversion ring decreases and the outer diameter of the diversion ring increases, the static pressure recovery coefficient of the exhaust cylinder will increase. When the initial diffusion angle is 15°, the outer diameter of the diversion ring The diameter is 5600mm, the streamline fits better with the diversion ring, the flow field distribution is stable, and the static pressure recovery coefficient is the largest; the optimization of the diversion ring structure can increase the static pressure recovery coefficient of low pressure exhaust steam by 37.1%, and the total pressure loss coefficient Reduced by 39%, the exhaust steam performance is better.

Key words: exhaust cylinder; guide ring; turbine; Finite Element

1

2

600MW

0.1

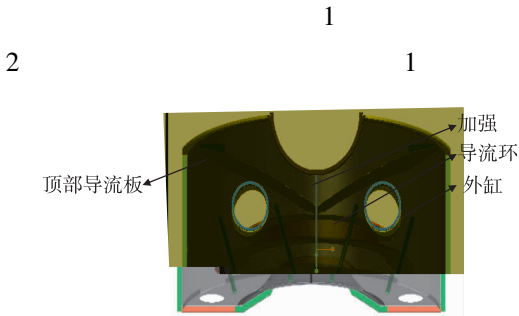
0.1% ~ 0.15%³

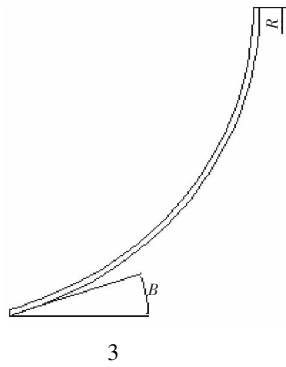
2020 - 08 - 27

1986 - 2012

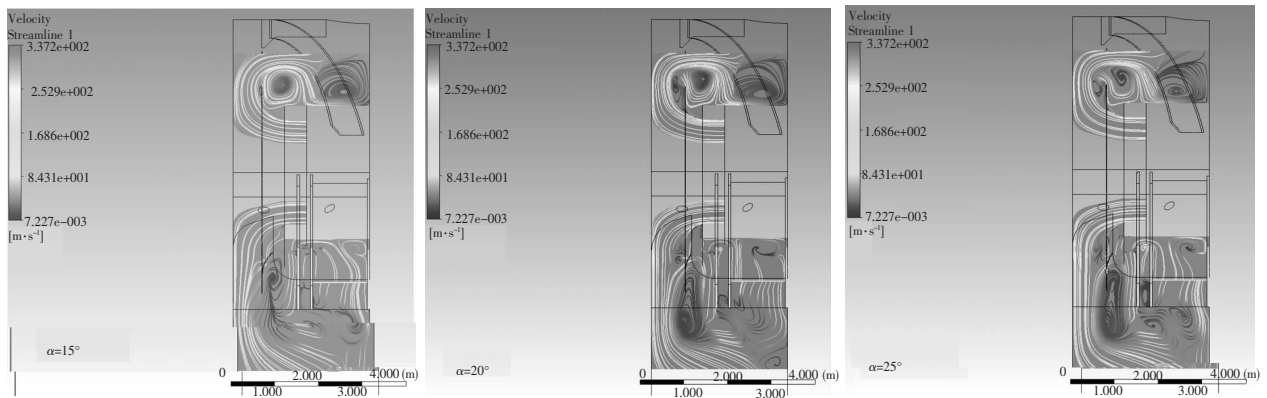
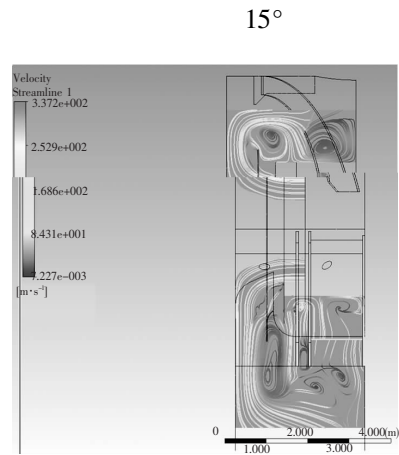
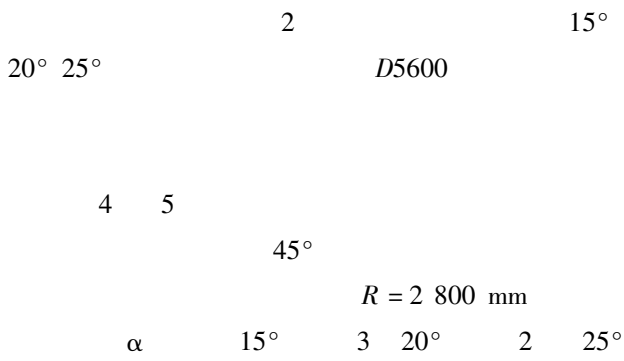
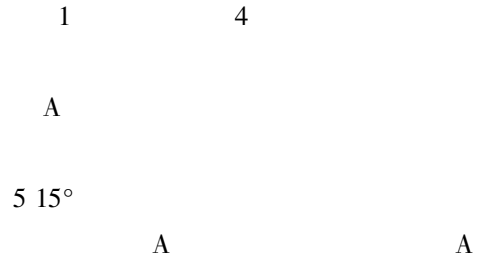
1

1.1





2.1



5

2

	1	2	3	
$/\circ$	26	25	20	15
R/mm	2 600	2 800	2 800	2 800
P_{in}/Pa	13 083.3	12 893.7	12 523.8	12 147.7
P_{out}/Pa	13 026.7	13 028.2	13 024.2	13 022.4
$P_{O_{in}}/\text{Pa}$	15 099.4	14 949.4	14 647.1	14 342.5
$P_{O_{out}}/\text{Pa}$	13 307.7	13 228.8	13 275.7	13 248.2
	0.028	0.065	0.236	0.399
	0.888 7	0.837	0.645 9	0.498 6

2.2

$R2800\ R2384\ R2200$

3

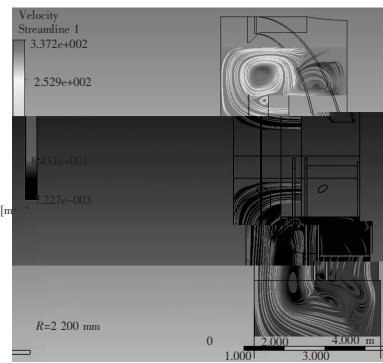
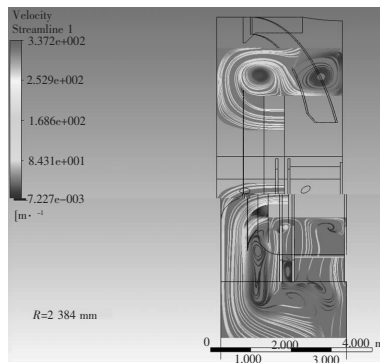
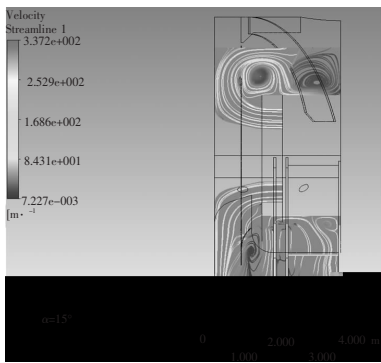
6

45°

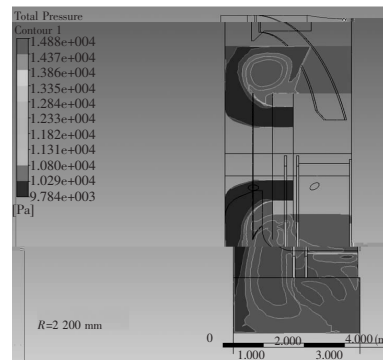
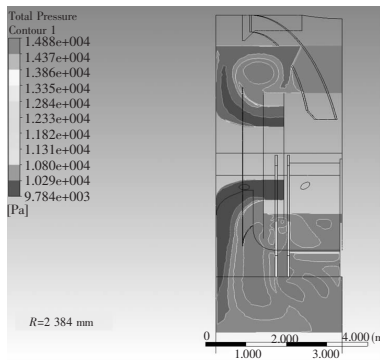
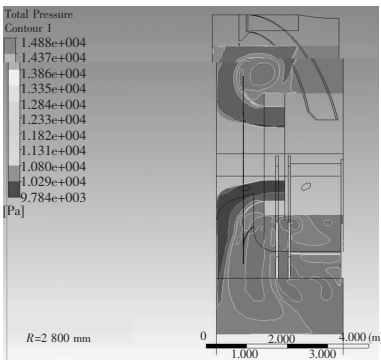
45°

15°
R = 2 800
3 2 384 mm 2 2 200 mm
1 R = 2 800 mm
3 A
2 1 A
7 2 800 mm

3
R = 2 800 mm 3
R =



6



7

3

	3	2	1
/°	26	15	15
R/mm	2 600	2 800	2 384 2 200
P_{in}/Pa	13 083.3	12 147.7	12 305.5 12 616.2
P_{out}/Pa	13 026.7	13 022.4	13 025.2 13 025.1
Po_{in}/Pa	15 099.4	14 342.5	14 460.4 14 7

4 7 1

UG

UG

TG659

A

1001-9006 2021 01-0049-06

Research on Multi-axis N/C Machining Technology of Open-integrated Impeller

WU Zhongjing, DUAN Changde, QIAO Jie, WU Wei

(Dongfang Electric Machinery Co., Ltd, 618000, Deyang, Sichuan, China)

Abstract: In this paper, for the NC programming of the open-integrated impeller, through the study of machining process, the processing procedure and the machining center, the tool selection strategy is determined. An efficient and optimal way of multi-axis NC programming is adopted based on the software of UG, and an experimental open-integrated impeller of high quality is produced, which proves the feasibility of the study.

Key words: integrated impeller; UG; multi-axis machining; NC programming

2

“3 + 2”

1

3

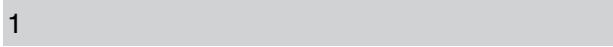
2020 - 12 - 25

1989 - 2011

1979 - 2002

1982 - 2011

1966 -



1
X

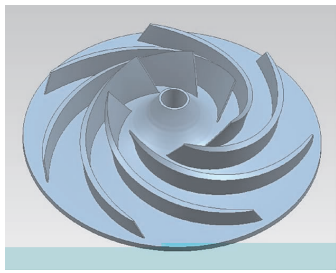


(a)开式整体叶轮 (b)半闭式整体叶轮 (c)闭式整体叶轮

1

1.1

2 7
1



2

1

mm

	582	50	/
	113	38	/
	13.2	3.5	10.7
	3	3	3
	6	6	6
	79	33	52.8

1

1

2

3

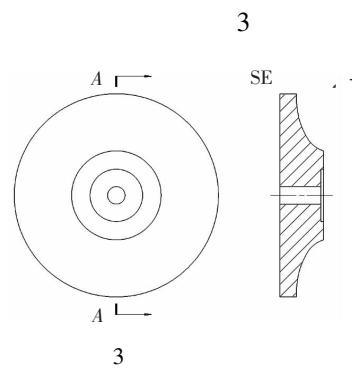
4

5

Ra 3.2 μm

± 0.2 mm

1.2



3

3

①

②

③

④

⑤

6

⑥

2

mm

<i>D52R5</i>	155
<i>D25R5</i>	220
<i>D20R10</i>	160
<i>D16R8</i>	160
<i>D12R6</i>	168

1.3

582 mm

CW6163C

2.2 UG

UG PRO-E

Cimatron MasterCAM

Open Mind

Hyper

mill

Concepts NREC

MAX-PAC

DMG

DMU 125P

4

XYZ

A

C

UG NX7.5

Unigraphics

UG

CAD/CAM/

CAE

/

/



4 DMU125P

4

UG NX7.5

1.4

2.1

D20R10

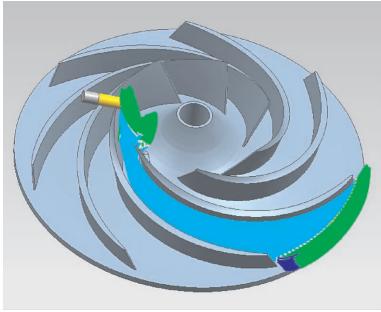
D16R8

6 mm

D12R6

2

5



5

finish

D20R10

UG blade_

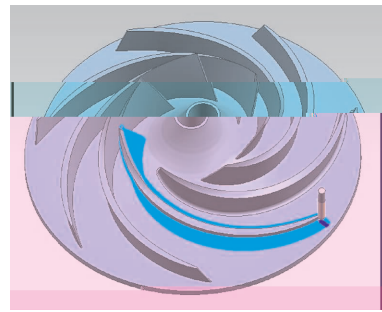
7

cavity_mill

D52R5

D25R5

3 + 2



7

variable_contour

6

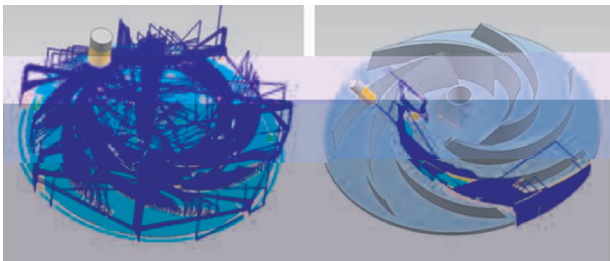
IPW in process workpiece

IPW

IPW

U V

6-7



(a)D52R5 粗加工刀轨

(b)D52R5 二次开粗刀轨

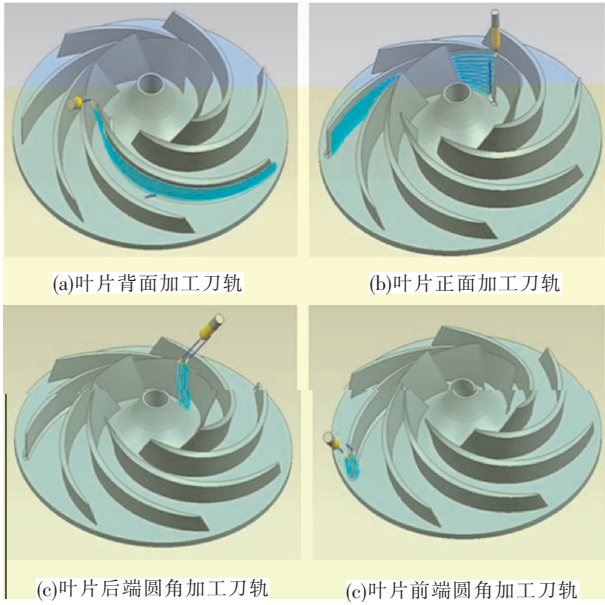
6

"3 + 2"

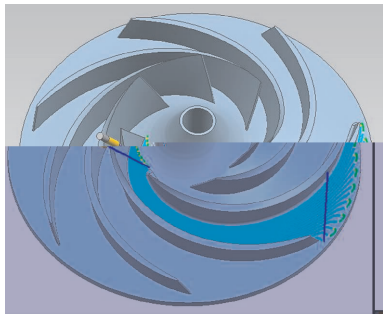
8

2.2

9



8



9

"3 + 2"

2.3

D16R8

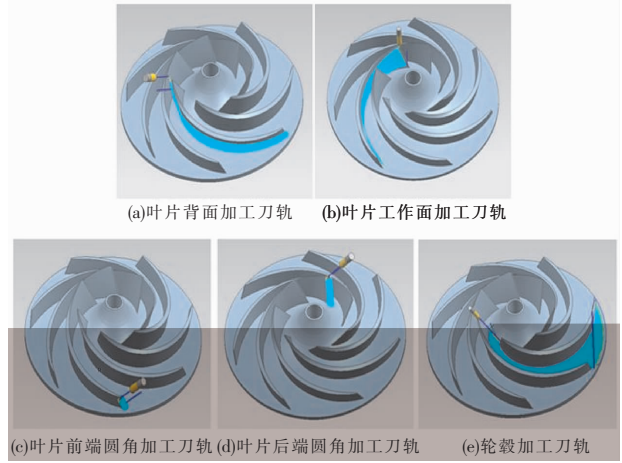
2.4

10

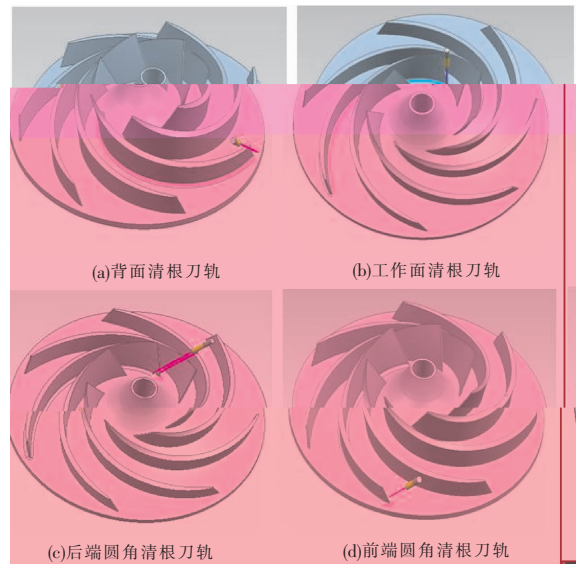
6 mm

D12R6

11



10



11

3

①

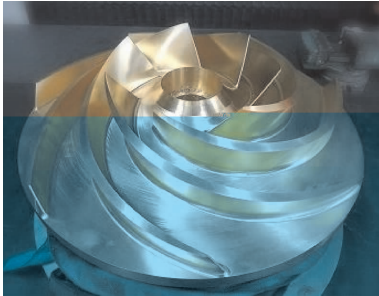
"3 + 2"

②

③

3

12



12

Ra3.2 μm

3

3

mm

	0.152 1	0.016 3	0.064 8
X	0.174 8	0.013 5	0.036 1
Y	0.152 1	0.010 6	0.030 7
Z	0.136 7	0.002 5	0.044 2

0.064 8 mm

± 0.2 mm

4

UG

- 1 . J . 2014 2 31-38
- 2 . D . 2017 3-4
- 3 . M . 2011 8-9
- 4 . M . 2011 6-7
- 5 . UG NX6.0 M . 2010 1
- 6 . UG J . 2008 1 25-26
- 7 . UG J . 2007 8 4 40-44

48

R2800

3

15°

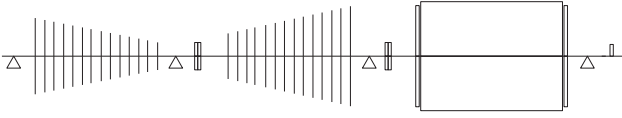
R2800

37.1%

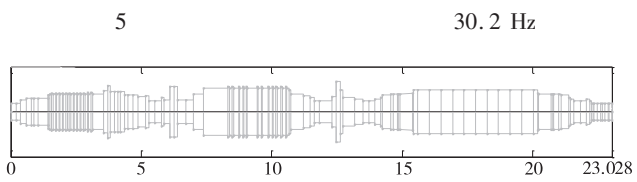
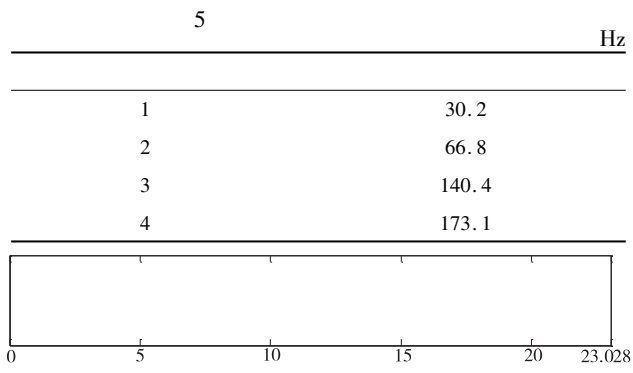
39%

4

- 1 . J . 2002 2 1-6
- 2 . J . 2018 2 7-12
- 3 . 600 MW J . 2017 38 2 41-43



5 5 ~ 8



	1	1	2
1.		618000 2.	618000

TM614

A

1001-9006 2021 01-0058-03

Research on Acquiring Experimental Data Acquisition System for Wind Farms

XU Fuxia¹, LI Yuxia¹, CHEN Feng²

(1. Dongfang Electric Wind Power Co., Ltd., 618000, Deyang, Sichuan, China;

2. Dongfang Turbine Co., Ltd., 618000, Deyang, Sichuan, China)

Abstract: Based on the needs of experimental data collection, an automated data collection tool is studied in this paper. Through experiment demand data collation, and relying on the demand on the collection tool, the relevant demand data is automatically obtained through the collection tool, including historical data, without human intervention. The results show that this automatic collection tool makes data collection more convenient, smarter and simpler. The data collection tool fully meets the laboratory's requirements for experimental data, and is configured and selected according to needs, which is important for the efficient acquisition of data.

Key words: experimental data; acquisition tool; automation; intelligence

4. 0

①

②

③

2020 - 06 - 29

1980 - 2006

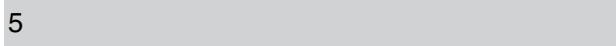
2

3

4



5



1



2021 1 31 23

6

15

"

"

"

"

"

"

"

"

6 300 MW

-

650 m

"

"

21.6

47.5

1.079

2.879

"

"

"

"

"

"

来源:东方电气网

TRIZ

618000

TRIZ

TRIZ

TM614

A

1001-9006 2021 01-0061-04

Application and Discussion of TRIZ Theory in Improvement of Yaw System of Wind Turbine

SUN Zhongze, SU Ninglie, YANG Xiaolin

(Dongfang Electric Wind Power Co. , Ltd. , 618000, Deyang, Sichuan, China)

Abstract: In the yaw system design of wind turbines, according to the design of driving load, the strength of outer teeth of bearing and driving teeth is often insufficient, especially for motor starting conditions. Therefore, it is often necessary to consider increasing the number of drivers, or increasing the tooth width, which increases the cost. Based on the innovative methodology of TRIZ, brainstorming is carried out to optimize and improve the driving structure in a directional way, and many new schemes are obtained for evaluation and verification by design engineers. In this paper, the yaw system of wind power is taken as the object to discuss the methodology for reference in other fields.

Key words: TRIZ; innovative method; wind turbine; yaw system; tooth surface

TRIZ

1

1.1

2.2

1

2

3

+

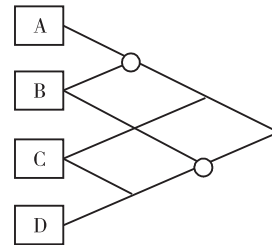
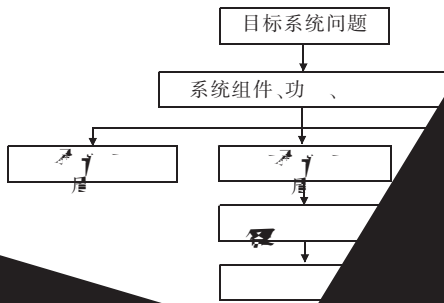
1.2

1

RIZ

ABCD

3



2

控制 → 驱动电机

↓ 减速箱

↓ 驱动齿

↓ 偏航轴承齿

支撑

机舱

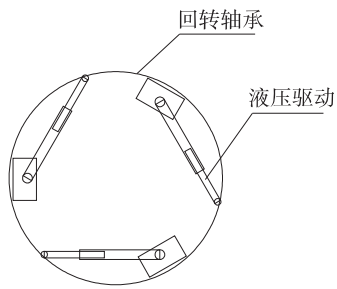
40 "

"

2

3

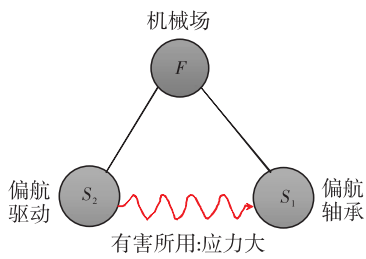
6



6

4.2

7



7

1

No. 15

"

"

8

偏航驱动

偏航

气动力场



618000

CFD

TM612

A

1001-9006 2021 01-0065-05

Analysis and Research on Guide Vane Water Leakage in Large Francis Hydro-turbine Unit

SONG Min, LI Haoliang, ZHANG Hong

(DongFang Electrical Machinery Co. Ltd. , 618000, Deyang, Sichuan, China)

Abstract: The guide vane water leakage strongly influenced the water energy utilization, effective operation, material damage and other issues of hydro-turbine. Thus, the guide vane water leakage is an important factor for hydro-turbine, which is usually measured in prototype tests but lack of prediction, analysis and optimization methods in design stage. Based on the structural statics and CFD finite element analysis (FEA) method and theoretical computation, this study analyzes the water leakage at guide vane vertical-surface gap with different trailing-edge shapes and the water leakages at flange plate gap. Results show that the optimum guide vane scheme obviously Sid

S Sa e en e a o n

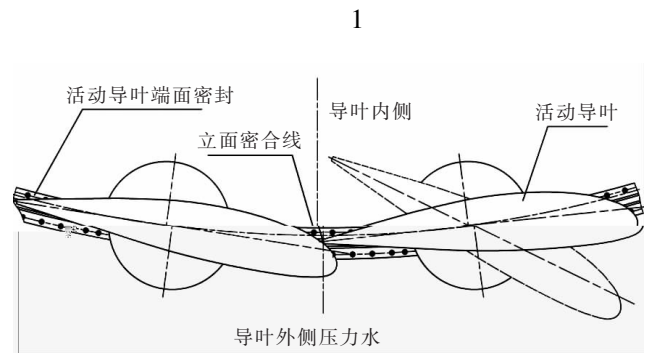
2020 – 12 – 25

1979 – 2002

1986 – 2011

1991 – 2014

1-3

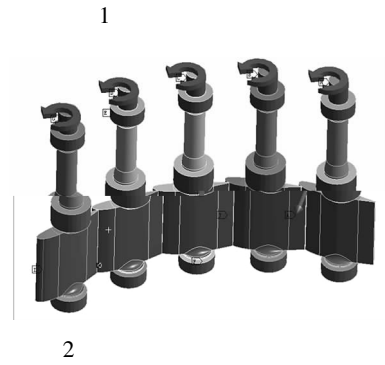


5

7

4

6



2

8-10

CFD

+

1.2

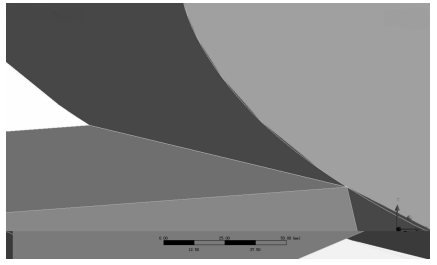
3

1

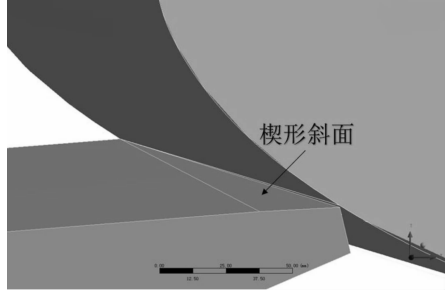
1.1

24

4

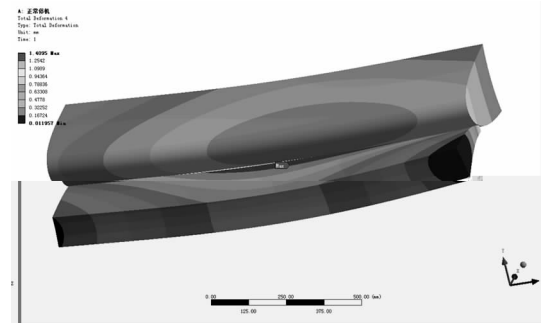


3



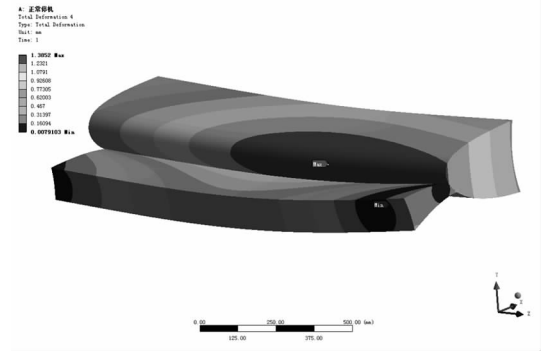
4

1.3



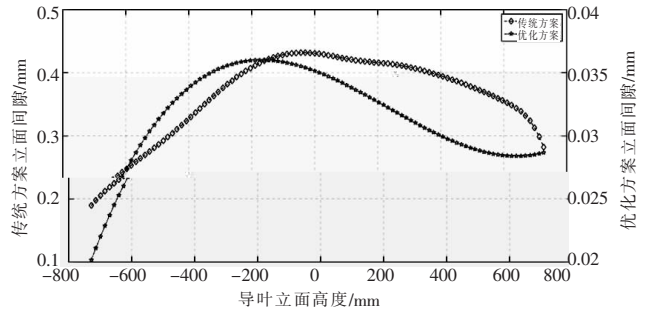
5

58



6

58



7

Q_z

11

5 6
58

$$Q_z = \mu \sqrt{2g \cdot \Delta H} A = \mu \sqrt{2g \cdot \Delta H} \sum_{i=1}^{24} A_i \quad 1$$

$$\mu \quad A \quad g$$

ΔH

24

24

Q_z

1

496.31 mm²
46.13 mm²

0.465 9 m³/s
0.043 3 m³/s

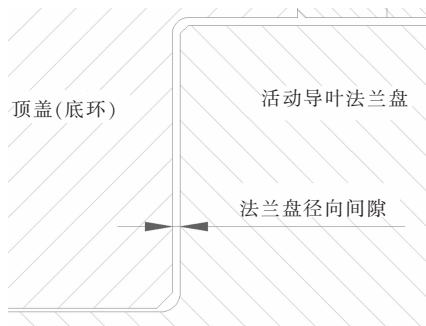
9.3%

1		
	/mm ²	/m ³ ·s ⁻¹
11 911.44		0.465 9
1 107.12		0.043 3

2

8

a mm
mm $2a$ mm $3a$ mm



8

$$Q_f = b_1 h_f + b_2 \quad 2$$

Q_f m³/s
 h_f mm

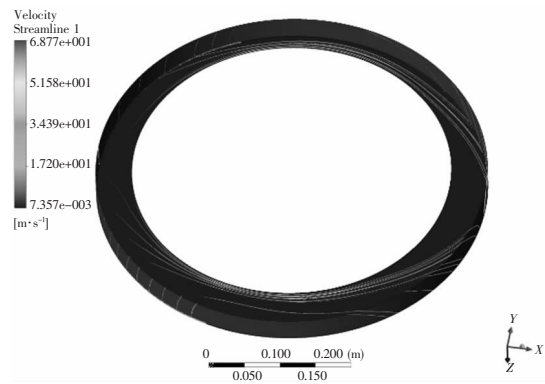
$$Q_f = b_1 h_f + b_2 \quad 2$$

b_1 b_2 $b_1 = 0.204 3$ $b_2 = 0.051 8$

2

m³ s⁻¹

a mm	5.269 3E -03	0.252 9
$2a$ mm	9.727 9E -03	0.466 9
$3a$ mm	1.378 1E -02	0.661 5



9

a

3

$2a$ mm

0.465 9 m³/s
m³/s 0.93 m³/s
0.97 m³/s

4

1 Li D Gong R Wang H et al. Analysis of vorticity dynamics for hump characteristics of a pump turbine model J . Journal of Mechanical Science and Technology 2016 30 8 3641 -3650

2 J . 2014 32 11 927 -930

3 Yao Y Xiao Y Zhu W et al. Numerical analysis of a model pump-turbine internal flow behavior in pump hump district C . IOP Conference Series Earth and Environmental Science 2014 22 3 032040.

4 GB/T 15468 -2006 S .

5 J . 2010 30 4 11 -13

6

J . 2016 10 9 -10

7 J . 2008 3 34 -37

8 Zhang D S Shi W D Chen B et al. Unsteady flow analysis and experimental investigation of axial-flow pump J . Journal of Hydrodynamics Ser. B 2010 22 1 35 -43

9 Rivetti A Lucino C Liscia S et al. Pressure pulsation in Kaplan turbines Prototype-CFD comparison C . IOP Conference Series Earth and Environmental Science 2012 15 6 062035

10 J . 2005 41 5 38 -43

11 J . 2016 42 11 76 -79

12 J . 2014 8 63 -66

64

2

1

2

3

4

5

6

7

8

5

TRIZ

8

TRIZ

1 TRIZ

M .

2015. 10

2

D .

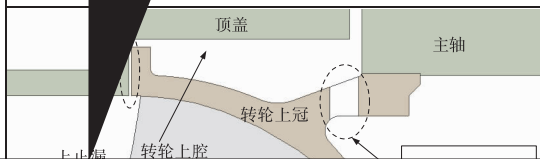
2011

2020 - 12 - 25

1977

-

16 D100



$$P_k = \mu_i \left(\frac{\partial \mu_i}{\partial x_j} + \frac{\partial \mu_j}{\partial x_i} \right) \frac{\partial \mu_i}{\partial x_j}$$

$$C_{2\varepsilon} = 1.92 \quad k = 1.0 \quad \varepsilon = 1.3$$

2.2

1/12

1/

16

2

214 rpm

2.1

10^{-5}

2

Dout

1

Ain

N-S

4/3

5

CFD

ANSYS-CFX

k-

6

$$\frac{\partial}{\partial t} + \frac{\partial (u_j)}{\partial x_j} = 0$$

1

$$\frac{\partial (u_i)}{\partial t} + \frac{\partial (u_j u_i)}{\partial x_j} = -\frac{\partial p'}{\partial x_i} + \frac{\partial}{\partial x_j} \left[\mu_{\text{eff}} \left(\frac{\partial u_i}{\partial x_j} + \frac{\partial u_j}{\partial x_i} \right) \right] + g_i$$

2

k

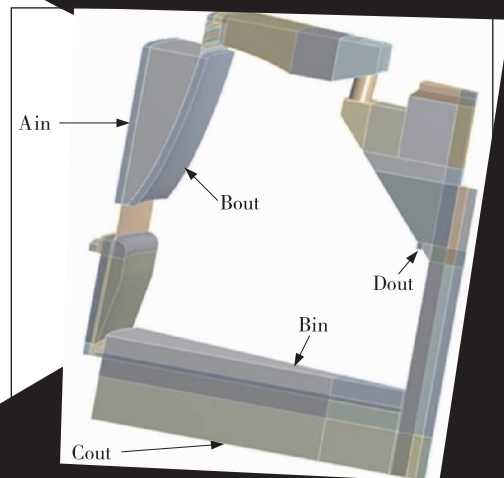
$$\frac{\partial}{\partial x_j} \left[\mu_j k - \left(\mu + \frac{\mu_i}{k} \right) \frac{\partial k}{\partial x_j} \right] = P_k -$$

3

$$\frac{\partial}{\partial x_j} \left[\mu_i \left(\mu + \frac{\mu_i}{\varepsilon} \right) \frac{\partial}{\partial x_j} \right] = \frac{C_{1\varepsilon} P_k}{k} - C_{2\varepsilon}$$

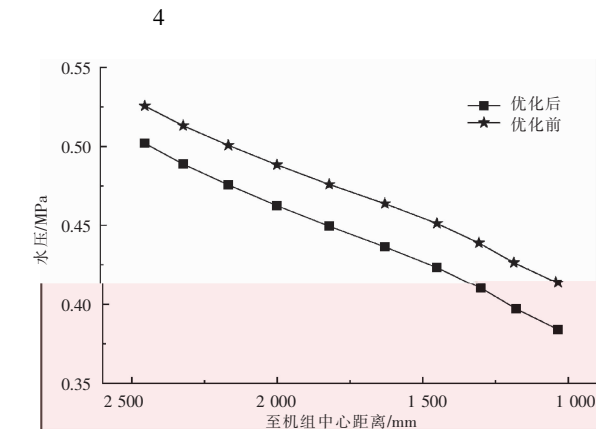
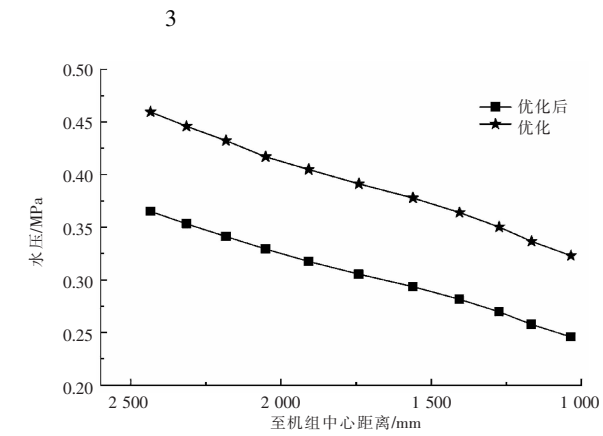
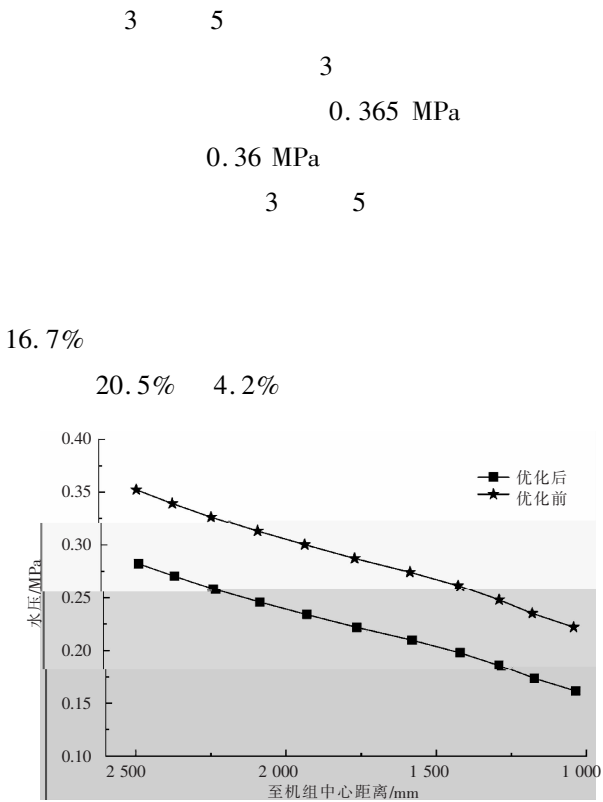
4

$$u_i = C_\mu \frac{k^2}{\varepsilon}$$



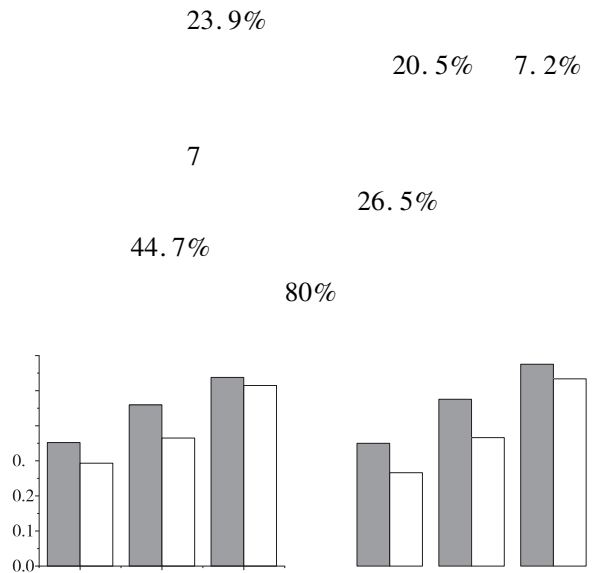
Ain	/kg s ⁻¹	22 155	20 872	19 110
Bin	P ₁ /MPa	0.166	0.175	0.365
Bout	P ₂ /MPa	0.528	0.696	0.712
Cout	V/m s ⁻¹	13.135	12.374	11.330
Dout	P ₃ /MPa	0.094	0.163	0.352

3



5

6





618000

?

1

2020 - 12 - 25

1989 - 2011

12

2.1.1

1 4

1-5

6-9

1.2

42

4

4

168

20

mm

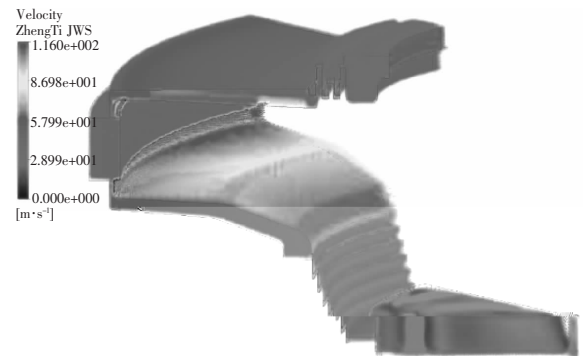
42

42

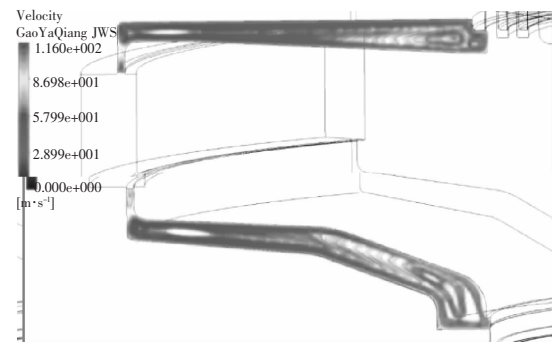
2

10-11

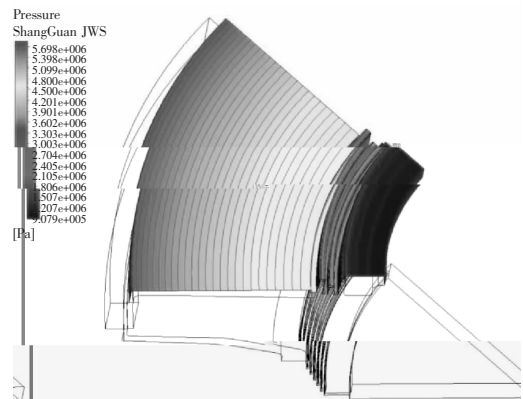
10



1

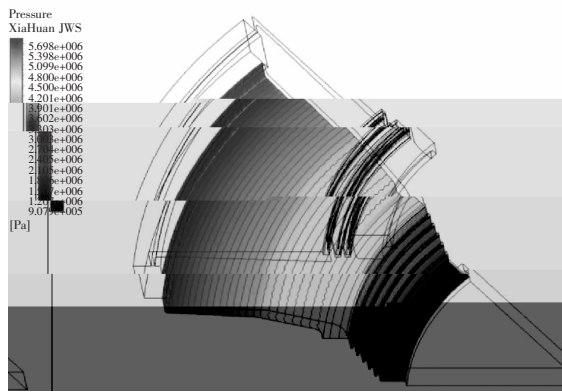


2



3

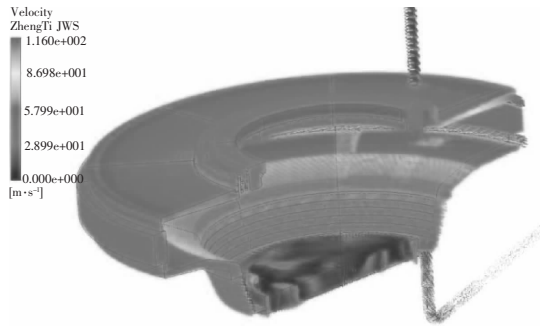
2.1



4

2.1.2

5 8



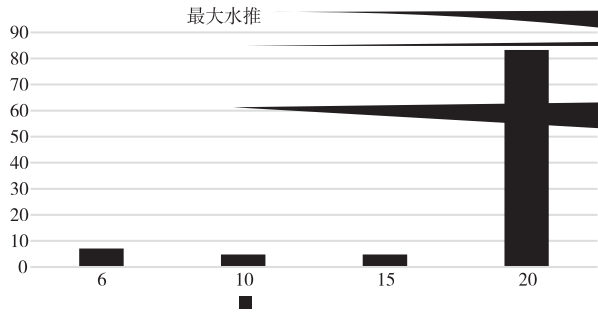
5

4.8%

20 mm 35

83.3%

10



	1	2	
1.		610000 2.	611731

TP391

A

1001-9006 2021 01-0077-08

Survey of Alarm Correlation Analysis for Communication Networks Based on Machine Learning

DING Hong¹, ZHOU Honglin²

(1. China Mobile Group Sichuan Co., Ltd., 610000, Chengdu, China; 2. DEC Academy of Science and Technology Co., Ltd., 611731, Chengdu, China)

Abstract: Alarm correlation analysis is the main technology for fault management in telecommunication networks. By means of alarm correlation analysis, the network maintainer easily reduces the redundant alarms and locates the root alarm. It is also one of the key technologies for AIOps. Therefore, it is significant to summarize the procedure and algorithm for alarm correlation analysis. As a first step, this paper introduces the general procedure for machine learning-based alarm correlation analysis in telecommunication network. In the following, the current research status for several key steps like alarm preprocessing, correlation analysis algorithm, and correlation rule generation are introduced and compared in detail. Then, the implementation of alarm correlation analysis based on big data processing framework has been summarized. Finally, the conclusion is drawn and the future research direction of alarm correlation analysis is also proposed.

Key words: alarm correlation analysis; correlation rule mining; machine learning; data mining; fault management

5G

2020 - 09 - 15

1983 - 2009



5

4

K-Means

5 DBSCAN⁶

2.1

7

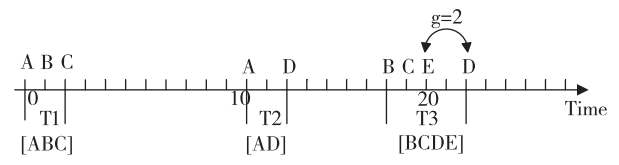
3

g 2

2

2 3

T1 T2 T3

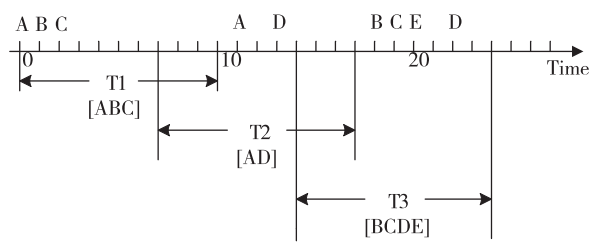


3

A-E 2 10 7
 3 3 T1

2.2

T2 T3



2

3

8

	3			
	9	15	K - Means	
				16
	10			
	3			
11			17	
3				
SVM AHP	12			
3				
		13		
		3		
		K - Means		
				18
	14			
3				
SVM AHP3				
AHP				
AHP				
SVM				
2.3				3
				1

2

3

3

Apriori

Apriori

2000 Apriori Han
FP-Growth
Apriori

1 -

FP-Tree

FP-Tree

1 -

FP-Tree

22 FP-Growth

3.1

FP-

Apriori¹⁹ FP-Growth²⁰ Eclat²¹ Apriori Growth

4

FP-Growth

FP-Tree

WFPF-Tree

N

N -

A

B -> A-B

WFPF-WARM

B

A

A

B

FP-Growth

Apriori

3.2

1 -

2 -

4 DFS-RG'

5

Hadoop³² Spark³³ Hadoop
HDFS
MapReduce
Map Reduce
34 Hadoop Apriori
VMSPA
SAAP³⁵ MSPA³⁶
37 FP-Growth
PFP³⁸ Hadoop
CanTree Hadoop
Spark Hadoop
RDD
Hadoop 100 Mlib Spark
?

- 3 . D .
2012
- 4 . D .
2010
- 5 . D .
2016
- 6 Chehreghani M H Abolhassani H Chehreghani M. H. Improving density-based methods for hierarchical clustering of web pages J . Data & Knowledge Engineering 2008 67 1 30 -50
- 7 Lozonavu M Vlachou-Konchylaki M Huang V Relation discovery of mobile network alarms with sequential pattern mining C // International E. oprV

n

s



611731

“ ” “ ” “ ” “ ”

360

C931.2

A

1001-9006 2021 01-0085-04

Application Research of Honest Risk Prevention and Control In Post Work Flow

JIANG Lina, CHEN Jian, ZHAO Xiaobo, LONG Yuting

(Dongfang Electric Co., Ltd., 611731, Chengdu, China)

Abstract: The discipline inspection has not been in a passive situation any more, when honest problems piled up and negative impact revealed. Nowadays, the honest risk prevention and control is more developed, getting on the root and concerning more on the prevention and long-acting. Sorting out the post work flow and rules and regulations process overall, investigating the potential honest risk, grading the honest risk and making prevention and control measures. Then the honest risk for each post and each work flow could be reduced to the low level with power exercised in the institutional cage and locked in the work process chain. The article describe this innovative working methods in detail, analyze, summarize and share the working experience.

Key words: honest risk; post work flow; rules and regulations process; prevention and control measure

2013 1

“ ” “ ” “ ”

“

360

“

“

“

“

“

1

“

“

2020 - 10 - 14

1983 - 2005

“ ”

”

”

2

”

”

3

20

“ ”

5.1.3

1

“ ”

4

“ ”

2

2

PDCA

5

5.1

5.1.1

5.1.2

6

84				15-23
36	J .	MapReduce Apriori	2014 13 4 411-415	38 Mao Weijun Guo Weibin. An improved association rules mining algorithm based on power set and Hadoop C //Proc of International Conference on Information Science and Cloud Computing Companion 2013 236-241
37	J .	PFonCanTree MapReduce	2018 40 1	



2021 2 19

2020

" 2020

"

2018

2018 ~ 2020

2.68

50

18

1

60%

100%

2019

2020

"

2020

"

"

来源:东方电气网